The Long-Run Effects of Coal-Fired Power Plants on Health in India *

Raahil Madhok[†] University of Minnesota
Rohini Pande[‡] Yale University
Kevin Rowe[§] Uber
Anish Sugathan[¶] IIM Ahmedabad

March 01, 2023

Abstract

This paper quantifies long run health effects of India's expansion of coal-fired power plants from 1970 to 2017. We use a particle trajectory model to build an exogenous measure of cumulative exposure to power plant emissions over several decades. This measure predicts present-day air quality substantially better than conventional wind direction-based measures. A one standard deviation increase in long run exposure to power plants increases neonatal, infant, and child deaths by 2% each. We find no evidence of differential economic development between more and less exposed districts, ruling out adaptation and underscoring pollution as the main mechanism. A plant-level investigation reveals older, inefficient plants drive the bulk of mortality effects. Counterfactual simulations suggest that taking these plants offline can avoid 18,000 child deaths over the next thirty years.

[†]rmadhok@umn.edu
[‡]rohini.pande@yale.edu
[§]roweke@gmail.com
[¶]anishs@iima.ac.in

1 Introduction

Increased electricity demand is an emblematic feature of economic development. A third of global electricity is generated by coal power plants, with China and India accounting for 85% of installed capacity (Shearer et al., 2019). While electricity catapults economic progress, coal combustion also releases harmful air pollutants. In 2015, outdoor air pollution led to 4.5 million deaths worldwide (Landrigan et al., 2018; Murray et al., 2020). Nearly 1 million of these occurred in India.

The short term impacts of poor air quality is well studied, but less is known about the long term due to difficulty finding quasirandom variation in long term air quality across geographic units. A deeper understanding of the long run is necessary since most pollution regulations strive for long run improvements in air quality. Many dominant air pollution sources, like power plants, are also long-lived infrastructure assets.

This paper documents the impact of long run exposure to coal-fired power plant emissions on early-life mortality in India. Power plants are the largest point source of outdoor air pollution in India. Despite recent growth in solar capacity, India remains reliant on coal to supply two-thirds of its electricity. Even if investment in coal-fired power stopped today, it is projected dominate the grid until 2040 (International Energy Agency, 2021). This inertia reflects over five decades of concerted investment in coal-fired electricity.

A key challenge for answering our question is finding long-run variation in exposure to power plant emissions at small spatial scales. Two short-run studies set the stage. Barrows et al. (2019) find that a 1 standard deviation increase in coal power plant capacity in Indian districts results in 15% higher infant mortality. The equivalent mortality impact is 6.5% in United States counties (Clay et al., 2016). Both studies leverage annual panel data over several decades. Extrapolating to the long-run is problematic because of non-linear dose-responses such that the cumulative impact of long-term exposure exceeds the sum of short-term coefficients. What is needed, rather, is a direct source of exogenous variation in long-run exposure to coal power plant pollution.

We overcome this empirical challenge in two steps. First, we compile data on the locations and starting dates of all coal power plants built between 1970-2017. Second, we compute sptio-temporally explicit exposure to emissions from these plants using the HYSPLIT[1] air parcel trajectory and particle transport model. We setup the HYSPLIT model to compute the down-wind dispersion trajectories of particle plume emanating from each plant chimney, and geolocate the particle landing points to estimate the down-wind pollution concentration distribution. We run this model on a plant-by-week basis for 30 years and then compute cumulative exposure at the district level. This yields a novel, plausibly exogenous, measure of districts' population exposure to upwind power plant pollution.

[1]The Hybrid Single-Particle Lagrangian Integrated Trajectory (HYSPLIT) model developed by NOAA is widely used by researchers and emergency response personnel to establish source-receptor relationship for air pollutants and hazardous materials (Draxler and Hess, 1998; Draxler et al., 2020). We setup the HYSPLIT model to use the geo-locations of emission sources (power station chimneys) and the corresponding meteorology data: surface pressure or terrain height, u-v wind components, temperature, and moisture (RELH) (https://www.ready.noaa.gov/hysplitusersguide/S141.htm)

Our model-generated exposure measure predicts ambient pollution better than standard wind direction measures from the literature. Regressions of Nitrogen Dioxide (NO_2) concentration on historic power plant exposure yield F-statistics twice as large for our measure compared to wind direction based prediction. Our measure also has the advantage of imposing no restrictions on dispersion distance, enabling us to study health outcomes hundreds of kilometers away from the emitting plant.

To estimate long-term health impacts, we match power plant exposure with district mortality data from the Global Burden of Disease Study (GBD), which is the most comprehensive repository of neonatal, infant, and child mortality available to date (Dandona et al., 2020). These data are available for 2000, 2007, and 2017, permitting a research design based on three separate cross-district comparisons within states. This allows identification of plausible control groups for historically exposed districts: other districts in the same state, equidistant to the nearest power plant, but exposed to less of its pollution in the past three decades due to differences in wind fields.

Our first finding is that children in districts continuously exposed to coal power plant emissions over the past three decades experience significantly higher mortality rates in the first five years of life. A one standard deviation increase in historic exposure causes 2% higher neonatal, infant, and child mortality in the present day.

Second, we find significantly higher ambient SO_2 and NO_2 concentrations in districts historically more exposed to power plant emissions. This suggests that pollution is the key mechanism linking long run power plant exposure to health. As a placebo test, we estimate effects on PM2.5 levels, which is known to originate mainly from non-power plant sources. There is no statistical difference in PM2.5 between districts more- and less-exposed to power plant emissions.

Third, we find that long run health effects are less pronounced in urban areas. Ex-ante, the direction of heterogeneity is unclear. Urban districts may suffer worse exposure to the same power plant emissions due to higher population density. Yet, they also have better health infrastructure, mitigating health damages compared to rural areas. We interact cumulative exposure with population density and find that mortality is 20% *less* in population-dense districts. This suggests that an "urban advantage" protects the population, likely through better health care delivery.

Fourth, emissions exposure during the 2006-16 period is the critical period influencing present-day mortality. We arrive at this by unraveling cumulative exposure into distinct time bins in the cross-sectional regression. The result holds even when controlling for in-utero (short term) exposure, representing a "pure" long run response.

We find no difference in measures of economic development—including consumption per capita, service sector labour share, and nightlight intensity—between historically exposed and non-exposed districts, ruling out differential adaptation as a potential explanation for our results. Moreover, if healthy people move to less-exposed districts, then our results are overestimated. We find no evidence of different migrant shares between more- and less-exposed districts, ruling out endogenous sorting as a potential mechanism.

The paper concludes by formally studying policy implications. First, we replicate our main

mortality estimates at the plant level to identify which plants are the most damaging. We find that older, inefficient power plants are the culprit, many of which are located in Eastern India. Second, we conduct a series of counterfactual exercises to quantify the national benefits of alternative abatement scenarios in terms of avoided deaths. These scenarios include different percentages of installed capacity reduction as well as decommissioning vintage plants (25+ old) altogether. We find that a 25% reduction in coal-fired installed capacity (India's Paris Agreement Pledge) can avoid 3,300 child deaths. Retiring vintage power plants altogether avoids 18,000 child deaths. A map of these benefits shows that many avoided deaths occur in districts with no power plants, underscoring the positive externalities from abatement.

Literature Contributions. The primary contribution of this paper is to credibly estimate child health impacts of *long run* exposure to highly-emitting point sources of air pollution. Most related work documents *short term* health effects of air pollution in developed countries (Chay and Greenstone, 2003; Currie and Neidell, 2005; Currie and Walker, 2011; Knittel et al., 2016; Deryugina et al., 2019) and, to a lesser extent, in developing countries (Arceo et al., 2016; Jayachandran, 2009; Barrows et al., 2019). Among the few papers documenting long term effects, most elicit later-life impacts of early-life pollution exposure (Anderson, 2019; Rosales-Rueda and Triyana, 2019; Currie and Vogl, 2013). Besides studies focusing on in-utero exposure (Currie and Neidell, 2005; Von der Goltz and Barnwal, 2019), we are unaware of studies covering a longer historic period of exposure.

The second contribution is to provide new evidence on the long run health impacts of coal-fired power plants specifically. To our knowledge, no other study estimates health impacts of sustained exposure to power plants. Heblich et al. (2016) document path-dependence in UK neighborhood composition following historic power plant investments, but do not investigate health disparities. In the short run, Barrows et al. (2019), Cropper et al. (2021), and Gupta and Spears (2017) find increases in infant mortality and coughing incidence from power plant exposure in India. Our results imply that these adverse short term health outcomes are also observable in the long-run, implying minimal adaptation. This contribution is especially important given that coal is expected to be India's dominant fuel source for the next several decades.

The third contribution is our application of recent advances in atmospheric science to measure long run exposure to power plant emissions. We join an emerging literature using HYSPLIT to trace particle paths (Heo et al., 2023; Morehouse and Rubin, 2021; Hernandez-Cortes and Meng, 2023; Fowlie et al., 2023; Wen et al., 2023). Much of this uses HYSPLIT to measure transboundary pollution or convert source emissions to concentrations, whereas we use it to study health impacts. An exception is Heo et al. (2023), who use HYSPLIT to show that Chinese air pollution increases South Korean mortality. Our paper differs in two ways. First, we study domestic emissions and impacts. Second, we study effects of cumulative exposure to emissions over the long-run.

Reliance on HYPSLIT also enables improvements in causal inference. Previous studies compare treatment and control groups based on distance from a polluting source (Currie et al., 2015; Jayachandran, 2009; Komisarow and Pakhtigian, 2022) or wind orientation (Deryugina et al., 2019;

Barrows et al., 2019; Herrnstadt et al., 2021; Pullabhotla and Souza, 2022). Both approaches require restrictive assumptions about the radius of pollutant dispersal. Wind direction also loses explanatory power when aggregated. In contrast, our measure requires no assumptions about plume shape or size and retains all spatial variation during aggregation.

Methodologically, we join the literature using cross-sectional designs to elicit long-run impacts of environmental change (Mendelsohn et al., 1994). Most of these rely on a selection-on-observable assumption for identification, which is prone to omitted variable bias (Deschênes and Greenstone, 2007). Druckenmiller and Hsiang (2018) introduce spatial first differences to overcome this, however, comparisons are made between neighbours which is too restrictive for our application. Since our exposure measure is plausibly exogenous, conditional on controlling for site suitability, our approach is more flexible and less reliant on selection-on-observables.

Lastly, our paper is conceptually similar to studies that estimate negative externalities from endogenously placed infrastructure. Duflo and Pande (2007) study the impact of dams on agricultural in India using panel data and river gradient as an instrument for dam placement. Lipscomb et al. (2013) and Blakeslee et al. (2020) use similar data and approaches to study economic impacts of hydroelectricity and wells, respectively. Although we also use an underlying source of variation (i.e. HYSPLIT) for identification, our study differs in two ways. First, we elicit long-term impacts through cross-sectional comparisons. Second, we study exposure to power plant emissions, as opposed to the impacts of the infrastructure per se.

The rest of this paper is organized as follows. The next section describes the data and dispersion model. Section 3 outlines the research design and estimating equations. Section 4 presents the main results. Section 5 presents the policy analysis and Section 6 concludes.

2 Data and Measurement

Estimating health effects of long run exposure to coal power plants requires data on historic power plant construction, pollution, and child mortality. HYSPLIT draws wind-driven particle paths from each chimney in our sample to generate a measure of cumulative emissions exposure. This section describes these data and measurement procedures.

2.1 Data Sources

Power Plants. Thermal coal-fired power plants generate the lions share of India's electricity. We obtain annual capacity reports from the Central Electricity Authority (CEA) for the universe of utility-scale coal power plants commissioned between 1970-2017. There were 160 stations with 565 generating units (hereafter, power plants) operating during this time. We geolocate each plant and verify it with satellite imagery. Installed capacity is aggregated to the district level for analysis.

In the absence of data on decommissioning dates, we assume that plants live for approximately 30 years, which coincides with engineering estimates used by the CEA (Central Electricity Authority, 2020b). We also assume that plants operate at full capacity.

Figure 1: District-wise Neonatal Mortality (2017)

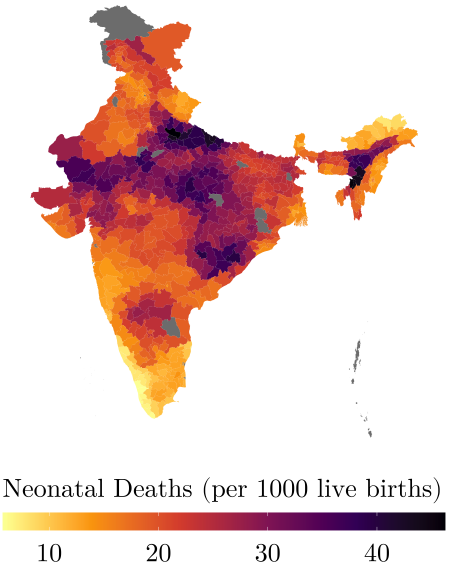

Note: Colours show neonatal deaths per 1000 live births from Dandona et al. (2020). Grey indicates NA.

Air Pollution. Monthly gridded SO_2 is retrieved for 2004-2017 from the Ozone Monitoring Instrument (OMI) aboard NASA's Aura satellite at $0.25 \times 0.25^{\circ}$ resolution. Grid cells show SO_2 concentration in the lower troposphere in Dobson Units (2.687×10^{-20} molecules$/m^2$). Gridded NO_2, measured in molecules$/cm^2$ for the same period, is also obtained from OMI. Both data products undergo substantial cleaning, validation, and outlier detection by NASA before public release.

$PM_{2.5}$ ($\mu g/m^3$) is derived from a reanalysis product developed by Van Donkelaar et al. (2016). $PM_{2.5}$ is an amalgamation of multiple particulate species and not measured directly by any satellite. The reanalysis data estimates $PM_{2.5}$ by assimilating concentrations of underlying particles (e.g. black carbon, organic carbon) through a geochemical transport model. Data is provided annually at 0.1×0.1 degree resolution for 1996-2017.

We construct a district-annual panel of all three pollutants in two steps. First, we extract weighted means across cells within 2011 district boundaries. Cells overlapping multiple districts contribute to each district mean in proportion to their overlap fraction. Second, we aggregate over months to the district-annual mean.

Neo-Natal, Infant, and Child Mortality. Mortality data is obtained from the Global Burden of Disease (GBD) project (Dandona et al., 2020), which, to our knowledge, contains the most comprehensive sub-national mortality estimates for India. District neonatal (0-28 days), infant (< 1 year), and child (< 5 years) deaths per 1000 live births are compiled for 2000, 2007, and 2017. Data are from many sources, including: Sample and Vital Registration System, Population Census, National Family Health Survey, District Level Household Survey, and Annual Health Survey[2].

[2]Data details are provided in Dandona et al. (2020).

Data are provided for 2017 district boundaries (723 districts). We map these back to their "parent" districts as per 2011 borders for consistent matching across datasets. Figure 1 illustrates the spatial distribution of neonatal mortality across districts in 2017.

Determinants of Plant Placement. Power plants are typically sited near water bodies and coal deposits (Section 3.2.1). These locations may develop differently than resource-poor areas. We select plant placement covariates based on engineering considerations and government guidelines (Central Electricity Authority, 2012, 2010; Mays et al., 2011; Planning Commission, 1961). Digital maps of coal deposits are obtained from the United States Geological Survey (Trippi and Tewalt, 2011). Rivers, lakes, and reservoir shapefiles are obtained at 10m resolution from Natural Earth Data.[3] A gridded digital elevation map is obtained from the NOAA at 10km $\times$ 10km resolution.[4]

We compute numerous covariates from these maps, including: distance from district centroid to nearest power plant, to nearest coal deposit, and to nearest water body.

Adaptation. We test for differential adaptation between districts more and less exposed to power plants using various economic indicators. Most are obtained from the Socioeconomic High-resolution Rural-Urban Geographic Dataset on India (SHRUG) (Asher et al., 2021), including: per capita consumption (Rs.), total employment in the service sector, and nightlight intensity. All variables are provided at the village/town level and then aggregated to the district.[5]

Residential sorting is another adaptation response that threatens identification (Kuminoff et al., 2013). We test for this using the newly released Census D3 migration tables, which report district migrant populations and when they arrived. We use number of migrants who migrated with their whole family to study endogenous sorting in section 4.6.

2.2 The HYSPLIT Particle Trajectory Model

This section describes our measure of long run power plant exposure used throughout the paper. It is computed by an atmospheric model that draws wind-driven particle trajectories from each chimney. The empirical strategy in Section 3.1 relies on this approach to generate exogenous variation in long run exposure to power plant emissions.

Overview. We use the Hybrid Single-Particle Lagrangian Integrated Trajectory (HYSPLIT) model developed by NOAA (Draxler and Hess, 1998; Draxler et al., 2020) to measure district exposure to power plant emissions. HYSPLIT can generate dispersion plumes from any point source by drawing wind-driven trajectories of air parcels emanating from the source—in our case, power plants. We use HYSPLIT because of its simplicity. More advanced chemical transport models (CTMs) estimate spatiotemporal pollution trajectories based on complex atmospheric chemistry at high

[3] Accessed from: http://www.naturalearthdata.com/downloads/10m-physical-vectors/

[4] Accessed from: https://www.ngdc.noaa.gov/mgg/topo/globe.html

[5] SHRUG draws from administrative data and maps to consistent geographic units. Underlying data for our variables include: 2012 caste census (consumption), 2013 Economic census (employment), and DMSP satellite (nighlights).

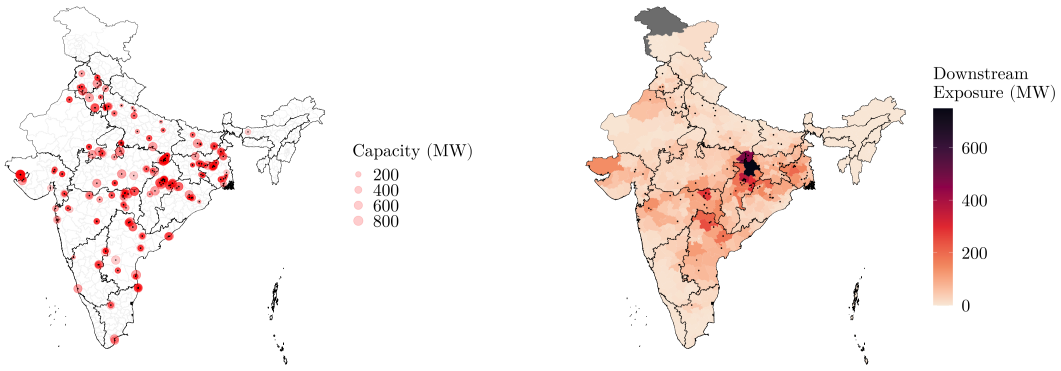

Figure 2: Coal Power Plant Capacity Expansion

A) Location and capacity of coal fired power plants in India (2017). B) Long-term cumulative capacity-weighted exposure estimated by the HYSPLIT model at the district-level (1987-2017).

resolution (Guttikunda and Jawahar, 2014). These require enormous computational power which make it impractical for studying exposure to hundreds of point sources over several decades. In contrast, HYSPLIT generates dispersion plumes almost entirely from 3D wind fields, which simplifies CTMs in exchange for computational scalability (Henneman et al., 2019, 2021).

Computation of Long-Term Exposure. We calculate long term exposure to power plant emissions in four steps. First, we generate a $0.1 \times 0.1^{\circ}$ grid and run the trajectory model for each power plant. Figure 2A shows the location and capacity of all 565 plants. The model emits a default number of tracer particles from the chimney for 24 hours every 30 days from the date of commissioning until 2017. After each 24-hour run, the count of particles landing in each grid cell measures the cell's exposure to the corresponding power plant. This process generates separate time-varying dispersion rasters for each of the 565 power plants in our sample describing the downstream count of tracer particles, $EmissionCount_{ijt}$, at each receptor grid cell i emitted from power plant j at time t.

Second, we normalize $EmissionCount_{ijt}$ to one and then sum over power plants in each year, adjusting for differences in installed capacity, $Capacity_{jt}$. This measures total exposure of grid cell i to emissions from *all* power plants operating in a given year, accounting for the fact that exposure to a large power plant is different than a small one:

$$GridExposure_{it} = \sum_{j} \left(\left(\frac{EmissionCount_{ijt}}{\sum_i EmissionCount_{ijt}} \right) \times Capacity_{jt} \right) \tag{1}$$

$GridExposure_{it}$ can be interpreted in MW equivalents, since the capacity of plant j is effectively distributed across the grid according to the exposure of each cell. Intuitively, if plant capacity is 1000 MW and the exposure of a far-away cell is 0.01, then it is as if there is 10 MW of installed capacity in the cell even though no power plant exists.

Third, we aggregate at the district level and accumulate to elicit long run exposure to power plant emissions. $CmlExposure_{dt}$ for district d between time $t-k$ and t measures district d's total

exposure (across all grid cells) to power plant emissions from historic period $t-k$ to the present:

$$CmlExposure_{dt} = \sum_{t-k}^{t} \sum_{i \in d} GridExposure_{i(t-k)} \tag{2}$$

The longest consistent cumulation window is thirty years since mortality is available for 2000, 2007, and 2017 and the oldest plant in our sample was built in 1970. Although the start year of cumulation differs in each year (i.e., 1970 for 2000, 1977 for 2007, etc), $CmlExposure_{dt}$ always refers to three decades of continuous exposure. This yields consistent coefficient interpretations in our regressions. Figure 2B shows the spatial distribution of $CmlExposure_{dt}$ for the year 2017.

Advantages of HYSPLIT-Generated Exposure Measure. Our measure of cumulative district exposure to power plant emissions offers several advantages that enable credible identification of long run impacts. First, it is entirely model-generated and requires no assumptions about shape and size of dispersion plumes. Conventional wind-direction measures assume a plume shape (typically a 45° cone around the wind vector) and length.

Second, since it is based on tracer particle counts (Equation 1), aggregation to any level retains all spatial and concentration information. This enables credible comparisons of health outcomes in exposed versus non-exposed districts. In contrast, conventional measures lose substantial explanatory power when averaged over multiple years (Section 4.2).

Third, since tracer particles are geotagged, we can cluster them into plumes. This allows us to correct for unobserved spatial correlation among districts under the same plume by clustering errors at the plume level (see section 3.1). This enables more precise estimation of standard errors.

Lastly, our approach enables meaningful counterfactual simulations. Since exposure is measured at the plant level, we can take plants offline or reduce their capacity, and then re-calculate cumulative district exposure (Equation 2) under various abatement scenarios. Section 5 estimates avoided deaths under alternative scenarios, including one where India meets it's Paris Pledge.

3 Research Design

This section describes our research design for estimating long run impacts of power plant exposure. We compare health outcomes in districts with different cumulative exposure to power plant emissions, controlling for geographic suitability for constructing the power plants. This design exploits cross-sectional variation, giving rise to plausible control groups for historically exposed districts: other districts with similar geographic characteristics, located equidistant to power plants, but historically less exposed to them due to plausibly random differences in wind fields.

3.1 Empirical Strategy

Estimating Equation. Since health data are for the years 2000, 2007, and 2017, we stack these cross-sections and estimate the impact of cumulative exposure to power plant emissions as follows:

$$Mortality_{dt} = \beta_1 CmlExposure_{dt} + \beta_2 \overline{X}_{dt} + \gamma_{st} + \epsilon_{dt}, \tag{3}$$

where $Mortality_{dt}$ is either neonatal, infant, or child deaths per 1000 live births in district d during year $t \in \{2000, 2007, 2017\}$. $CmlExposure_{dt}$ is defined in Equation (1) and measures cumulative exposure (in MW) to all upwind coal power plants in the past three decades (between $t-30$ and t) in district d. $\overline{X}_{dt}$, described in detail in the next subsection, is a covariate vector of site suitability metrics that account for the endogeneity of plant placement. State-year fixed effects, γ_{st}, ensure that cross-district comparisons are made within states separately in each of the three periods.

β_1 captures health impacts of district d being exposed to an additional MW of coal power plant emissions over the past three decades. Whereas location-by-time fixed effects typically identify short-term deviations, in this case β_1 is an average of three separate cross-sectional comparisons.

Identifying Variation. The site suitability vector, $\overline{X}_{dt}$, is key for identifying β_1. Whereas HYSPLIT draws wind-driven dispersion plumes, the existence of the plume itself is the outcome of an endogenous siting decision. After controlling for $\overline{X}_{dt}$, identification of β_1 relies on comparisons between districts with the same exposure *potential*, defined as having similar geographic suitability for plant placement and being equidistant to the nearest power plant, but some experience higher *observed* exposure due to plausibly random differences in wind fields (see Section 3.3 for illustration). Thus, the identification assumption is that cumulative exposure is orthogonal to other correlates of current health outcomes, *conditional on plant placement*. We discuss $\overline{X}_{dt}$ in detail, outline other identification threats, and visualize the empirical strategy next.

3.2 Threats to Identification

3.2.1 Endogeneity of Plant Placement

For decades, India prioritized siting power plants near coal deposits (Planning Commission, 1961) rather than near demand centers[6], known as the coal-by-wire policy. As we show next, this means that coal-proximate districts are more likely to have, and be exposed to emissions from, coal power plants. This poses an identification concern since these districts may be on different economic development paths compared to resource-poor districts *even in the absence of power plant exposure*.

[6]The 1961-66 Five-Year Plan states: "Steam power stations should be sited near collieries [coal mines], washeries [water bodies] and oil refineries. All power stations should be inter-connected to form state, zonal or super-grids, so that the energy is pooled and used to the best advantage of the region."(Planning Commission, 1961)

Table 1: Endogeneity of Power Plant Placement

	(1) Capacity	(2) Exposure	(3) Exposure	(4) Exposure	(5) Exposure	(6) Exposure
Distance to Coal (km)	-1.771*	-0.093*	-0.078**	-0.062**	-0.049**	-0.052*
	(0.956)	(0.046)	(0.037)	(0.028)	(0.022)	(0.029)
Nearest Coal Area (km^2)	-0.013	-0.003	-0.003	-0.002	-0.002	-0.004
	(0.048)	(0.003)	(0.003)	(0.003)	(0.002)	(0.004)
Water Area w/n 25km (km^2)	5.471	0.139***	0.096*	0.076	0.058	0.144
	(3.242)	(0.048)	(0.051)	(0.046)	(0.039)	(0.131)
District Area (km^2)	0.046***	0.002*	0.002*	0.002*	0.002*	0.002
	(0.009)	(0.001)	(0.001)	(0.001)	(0.001)	(0.001)
Elevation (m)	-0.374*	-0.009	-0.006	-0.004	-0.003	-0.005
	(0.184)	(0.005)	(0.004)	(0.004)	(0.003)	(0.004)
Slope (degrees)	40.326*	1.048	0.684	0.357	0.196	0.397
	(21.387)	(0.769)	(0.624)	(0.531)	(0.466)	(0.468)
Mask	None	None	10km	30km	50km	None
Plant District	Yes	Yes	Yes	Yes	Yes	No
Observations	640	640	640	640	640	532
R^2	0.121	0.384	0.424	0.455	0.478	0.358

* $p < .1$, ** $p < .05$, *** $p < .01$. All specifications include state fixed effects. Distance to coal (km) is measured from district centroid to nearest coal deposit. Nearest coal area and water area within 25km are means over district grid cells. The outcome in column 1 is cumulative installed capacity (MW) and in remaining columns it is capacity-weighted exposure cumulated over thirty years. Masks are the radius around power plants within which cells are deleted before aggregation. Column 6 drops districts with power plants. Standard errors clustered at the plume level.

The Coal-by-Wire Policy. We test for endogenous plant placement with the following equation:

$$Y_d = \mu_1 \overline{X}_d + \gamma_s + \epsilon_d \tag{4}$$

where Y_d is installed capacity or cumulative exposure in 2017. Other terms are the same as Equation 3. $\overline{X}_d$ is a vector of time-constant site suitability covariates, including: distance to nearest coal deposit, area of nearest coal deposit, water area within 25km, district area, elevation, and slope.

Table 1 show that districts close to coal receive more installed capacity (column 1), evidence of the coal-by-wire policy. These districts are also more exposed to power plant emissions in the long run (column 2). These findings highlight the need to disentangle placement- and wind-driven exposure to identify β_1 in Equation 3, since exposure through the placement channel is potentially correlated with health through natural resource proximity.

Isolating Exogenous Exposure. We address endogenous plant placement in two ways. First, we control for the site suitability metrics, $\overline{X}_{dt}$, directly in Equation 3. Second, we add masks with varying radius[7] to $GridExposure_{it}$ (Equation 1) before aggregating to the district level. We do this because the coal-by-wire effect in Table 1 is expected to weaken with distance since, at greater distances from coal and water, district exposure is more likely to be driven by exogenous wind

[7]The mask is applied by deleting cell values within 5-50km of the power plant.

fields rather than plant placement itself since the district is less suitable for a power plant.

Table 1 columns 3-5 show that the coal-by-wire effect declines with mask size. With a 50km mask (column 5), the correlation between exposure and coal drops by half whereas the correlation with water vanishes entirely. Column 6 takes a more extreme approach and drops power plant districts altogether. The correlation with coal nearly disappears ($p = 0.096$).

We acknowledge that applying a mask improves identification at the expense of excluding the most vulnerable population from the sample: those who live near and are most exposed to power plants. We present estimates with no mask and smaller masks to strike a balance between identification and sample composition.

3.2.2 Existence of Pre-Trends

Another threat to identification is the existence of pre-existing pollution trends. When the coal-by-wire policy is overlooked, power plants are sited near demand centres where ambient pollution may trend upward prior to plant placement. We address this concern in two ways. First, we control for distance from district d to the nearest power plant. Comparing equidistant districts helps ensures that they experience similar economic spillovers from the demand center.

Second, we formally estimate the dynamics of power plant placement and ambient air quality. We trace the path of ambient district pollution along the number of years each power plant has been active in a district with the following panel data model at the power plant level:

$$Log(Pollution_{dt}) = \sum_{\tau=-10/0}^{30} \beta_\tau D(t - e_{pdt} = \tau) + \overline{C}_{dt} + \alpha_p + \gamma_{st} + \epsilon_{dt} \tag{5}$$

where p indexes power plants, d indexes districts, s indexes states, and t indexes years. The outcome is log of ambient NO_2, SO_2, or $PM_{2.5}$. Pollution data are for 2004-2017 (section 2.1). e_{pdt} is the date that plant p was commissioned in district d. $\tau = 0$ is the reference period. $\overline{C}_{dt}$ are a set of covariates including rainfall, temperature, and installed capacity. α_p and γ_{st} are power plant and state-year fixed effects. We use the window $\tau \in [-10, 30]$ since this covers the pre-construction and end-of-life period for power plants. Each β_τ captures mean district pollution τ years relative to the date of commissioning. Non-existence of pre-trends is indicated by $\beta_\tau = 0 \ \forall \tau < 0$.

3.2.3 Spatial Correlation of Exposure

A final threat to identification is that exposure, pollution, and health are spatially correlated. Gridded exposure values (Equation 1) are spatially correlated through unobserved physics governing gas movement. An advantage of HYSPLIT is that we can demarcate boundaries within which spatial correlation is strongest, which we call a plume, and then cluster errors at this level.

We demarcate plumes using k-means clustering on each exposure grid (Equation 1), which identifies subgroups of cells with similar exposure values based on euclidean distance (MacQueen et al., 1967). We assign common cluster IDs to districts spanned by the same plume and those

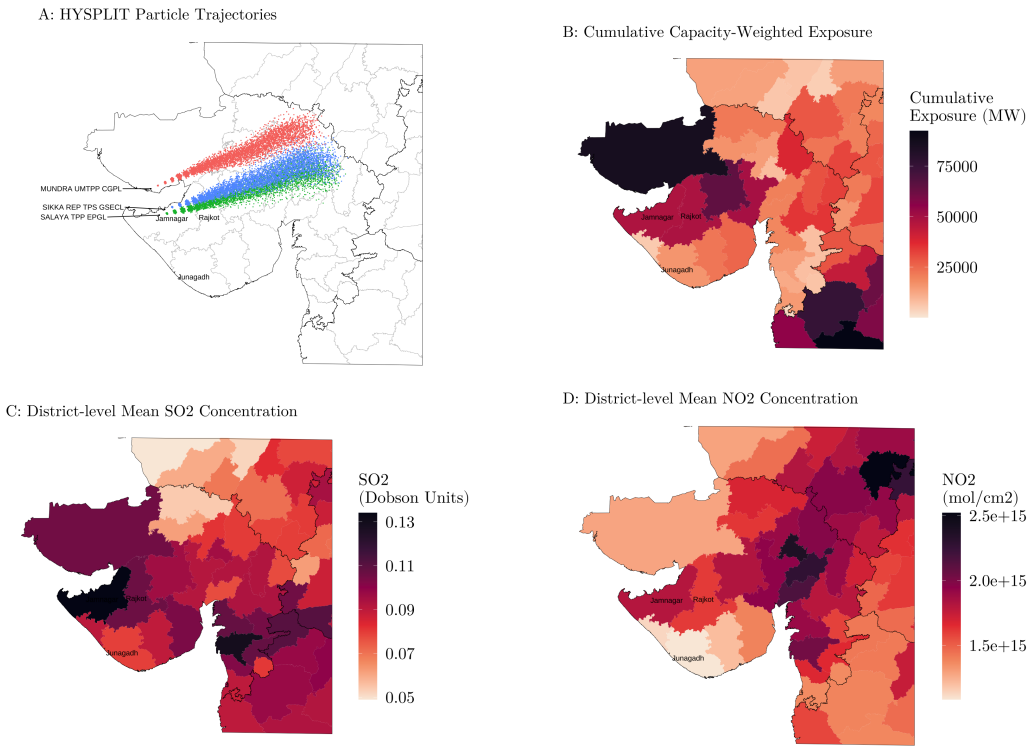

Figure 3: HYSPLIT particle trajectories, cumulative emissions exposure, and pollution.

Note: Example illustrations of HYSPLIT and pollution in Gujarat. Panel A shows HYSPLIT output from 24-hr run on April 2016 for three power plants in Gujarat. Panel B shows cumulative capacity-weighted exposure (2016). Panels C and D show district-level annual mean SO_2 and NO_2 concentration, respectively, for 2016.

spanned by multiple plumes are assigned the cluster with the highest overlap fraction. We demarcate 25 plumes for the main analysis (Figure A1) and test sensitivity in Section 4.5.

3.3 Visual Illustration of Empirical Strategy

Before turning to the results, we visualize our identification strategy. Consider the experience of Rajkot and Junagadh, the 4th and 7th most populous districts in Gujarat, respectively. They are also neighbours. Neither have their own power plant but both are approximately 150km from the nearest plant cluster (the Salaya and Sikka Power Stations) located in Jamnagar district. All three districts are thus expected to share similar site suitability for power plant placement.

Figure 3A shows that, despite similar exposure *potential*, proximity, and geography, Rajkot and Junagadh face drastically different exposure to the nearby power plants. Rajkot is directly in the exposure path of the Jamnagar plant cluster as well as that of the Mundra Ultra Mega Power Plant in Kutch district (red). Junagadh is completely non-exposed. These differences in exposure arise even when aggregating at the annual level (Figure 3B). It is this variation that we exploit to estimate the causal impact of power plant exposure. Figure 3C and D show that Rajkot's higher exposure translates into worse SO_2 and NO_2 levels, respectively. This is unsurprising since tracer

Table 2: Long Term Impact of Historic Exposure on Neonatal Mortality

	(1)	(2)	(3)	(4)	(5)	(6)
Capacity-weighted Exposure	0.300** (0.135)	0.438*** (0.136)	0.500*** (0.155)	0.516*** (0.167)	0.597*** (0.207)	0.650*** (0.221)
Nearest Plant	Yes	Yes	Yes	Yes	Yes	Yes
Geography Controls	No	Yes	Yes	Yes	Yes	Yes
Mask	None	None	5km	10km	30km	50km
Outcome Mean	29.071	29.071	29.071	29.071	29.071	29.071
Exposure SD	39.517	39.517	36.039	34.370	29.388	25.140
State × Year FEs	✓	✓	✓	✓	✓	✓
Observations	1920	1920	1920	1920	1920	1920
R^2	0.774	0.784	0.784	0.784	0.784	0.784

* $p < .1$, ** $p < .05$, *** $p < .01$. Data are district-year level for 2000, 2007, and 2017. Mortality measured per 1000 live births. Exposure is cumulative over 30 years and standardized. Geography controls include: distance to nearest plant, district area, water area within 25km, distance to nearest coal deposit, nearest coal area, elevation, slope, temperature and rainfall. Mask is radius within which exposure gridcells are deleted. Standard errors clustered by plume.

particles underlying the exposure measure largely follow wind patterns. In contrast, upwind districts like Junagadh experience lower pollution. These illustrations highlight the strong correlation between *model-driven* exposure and *observed* pollution. We show this more formally next.

4 Results

This section documents the health impacts of long run exposure to coal power plant emissions. We first report the main estimates and then investigate the extent to which pollution is the main mechanism. We also estimate heterogeneity by urban form and, lastly, unravel cumulative exposure to document the timing of health effects.

4.1 Main Results

4.1.1 Stacked Cross-section

Estimates of Equation 3 are presented in Table 2. The outcome is neonatal mortality and the explanatory variable, $CmlExposure_{dt}$, is standardized: a one unit increase corresponds to a one standard deviation (SD) increase in cumulative exposure. In column 1, distance from the district centroid to the nearest power plant is the only covariate. Although $\beta_1 > 0$, this is misspecified at larger distances since treatment and control districts are unlikely to share similar access to natural resources and may follow different counterfactual paths. Column 2 alleviates this by controlling for the site suitability covariates directly. The point estimate implies that an additional SD of emissions exposure over three decades causes 0.44 more neonatal deaths per 1000 live births, about 1.5% of the mean.

The remaining columns 3-6 explore sensitivity to various mask sizes. The mask serves to separate (endogenous) proximity-driven exposure from (exogenous) wind-driven exposure, although

in doing so, a vulnerable group is excluded from the sample. Mortality effects remain stable across 5-50km masks, with magnitudes ranging from 1.7-2.2%. These all fall within the 95% confidence interval of the estimate in column 2. The stable estimates suggest that the vulnerability of populations living near power plants is not too different than that of further away households. These findings imply that we can improve identification with a mask while maintaining sample representativity. We use a 50km mask for the remainder of the analysis.

Appendix Tables B1 and B2 present estimates for infant and child mortality, respectively. Across masks (columns 2-6 in both tables), effects range from 1.4-2.1% relative to the mean for infant mortality and 1.5-2.2% for child mortality. These results suggest that the long run mortality impacts of exposure to power plant emissions is similar for neonatal, infant, and child age cohorts.

As a sanity check, we calculate the contribution of historic power plant exposure to India's current neonatal mortality rate. Average district neonatal mortality declined from 36 to 22 deaths per 1000 live births between 2000-17. At the same time, the average district experienced 13 MW (1.9 SD) of cumulative power plant exposure. Table 2 column 6 implies that this led to 1.24 ($= 1.9 \times 0.650$) additional deaths, suggesting that the mortality decline in the average district suffered an 8.8 percent ($= 1.24/14$) setback due to cumulative exposure to power plant emissions.

4.1.2 Annual Cross-sections

Table B3 presents estimates of Equation 3 by year. Coefficient magnitude and precision are similar in 2000 and 2007 for all three outcomes, but decline in 2017. One explanation is that the lifetime of a coal power plant is around 25 years. Plants constructed in the 1980s would have gone offline between 2007-2017. Afterwards, pollution in downwind districts embodies less power plant emissions, leading to lower population exposure and smaller health impacts.

Event study estimates from Equation 5 are shown in Figure A2 and corroborate this explanation. Coefficients show district ambient pollution relative to the plant commission date. NO_2 and SO_2 concentrations are significantly higher throughout the plants' life compared to the pre-period. After 20 years of operation, NO_2 pollution declines towards pre-construction levels. After 25 years, there is no statistical difference between pollution in the pre- and post-periods.

4.1.3 Comparison with Short-Term Estimates

Although we focus on long run impacts, we also estimate short run impacts for comparison. This is interesting in its own right and also allows us to connect with the literature since, to our knowledge, there are no other estimates of long run mortality from power plant exposure. We measure short run exposure as $Exposure_{dt} = CmlExposure_{dt} - CmlExposure_{d(t-1)}$ and use $Exposure_{dt}$ to estimate Equation 3 by year. The resulting β_1 captures the impact of *contemporaneous* exposure to power plant emissions in year t on health in year t.

Table B4 presents the results. A 1 SD increase in short run exposure increases neonatal mortality by 6.6%, 9.4%, and 2.1% compared to the mean in 2000, 2007, and 2017 respectively (columns

Table 3: Impact of Historic Exposure on Log Pollution

	(1) Log SO2	(2) Log NO2	(3) Log PM2.5
Capacity-weighted Exposure	0.143***	0.076***	0.004
	(0.045)	(0.017)	(0.007)
Controls	Yes	Yes	Yes
Exposure SD	25.140	25.140	25.140
State × Year FEs	✓	✓	✓
Observations	1920	1920	1920
R^2	0.610	0.857	0.904

* $p < .1$, ** $p < .05$, *** $p < .01$. Data are district-yearly for 2000, 2007, and 2017. SO_2 and NO_2 are in Dobson Units. $PM_{2.5}$ is in $\mu g/m^3$. Exposure is cumulative over thirty years, includes a 50km mask, and standardized. Geography controls include: distance to nearest power plant, district area, water area within 25km, distance to nearest coal deposit, nearest coal area, elevation, slope, temperature and rainfall. Standard errors clustered by plume.

1, 4 and 7). The equivalent long run estimates (Table B3) are 3.2%, 3.6%, and 2.0%. Short run estimates are larger by a similar number of percentage points for infant and child mortality.

As an additional check, we compare our short run estimates with Barrows et al. (2019), the closest short run study from India. They use annual district data from 1996-2014, the cone-based measure of exposure, and two-way fixed effects to estimate the annual effect of power plant emissions on infant mortality. They find that a 1 SD increase in power plant exposure increases infant mortality by 5%. Within their study period, our short run estimates for infant mortality are 7.0% and 9.3% in 2000 and 2007, respectively (Table B4 columns 2 and 5). The discrepancy may be explained by our improved exposure measure or the fact that we do not use time variation.

It should also be noted that the Barrows et al. (2019) estimate of 5% is larger than our long run infant mortality estimates of 1.4-2.1% (Table B1 columns 2-6). This validates our earlier finding that short run impacts of power plant exposure are larger than long run impacts.

4.2 The Pollution Mechanism

Plant-level Event Study Estimates. We establish preliminary evidence that pollution is a mechanism by ruling out pre-trends. If plant placement was correlated with local demand, for example, then pollution would trend with district GDP even during the pre-period. Figure A2 shows event study estimates from Equation 5. Coefficient estimates 1-5 years prior to plant commissioning are statistically indistinguishable from zero, implying that the timing of plant opening is plausibly exogenous to unobserved determinants of pollution.

District-level Estimates. Table 3 presents estimates of Equation 3 with log pollution as the outcome. There is a large and precise effect of historic power plant exposure on local pollution. Columns 1 and 2 show that a one SD increase in historic exposure increases present-day SO_2 and NO_2 concentrations by 14.3% and 7.6%, respectively.

In column 3, the outcome is $PM_{2.5}$. This serves as a placebo test since coal power plants are not

a major source of $PM_{2.5}$ in India, whereas they are a major source of NO_2 and SO_2[8]. As expected, cumulative exposure has no impact on $PM_{2.5}$, suggesting that mortality effects in Table 2 are driven by power plant emissions rather than other pollution sources. Table B5 shows estimates by year. The pollution effect remains stable: higher SO_2 and NO_2 concentrations are observed in more exposed districts. Moreover, exposure continues to have no effect on $PM_{2.5}$ in either period, in line with the explanation that power plants contribute little to ambient $PM_{2.5}$.

Comparison with Literature. These results are reminiscent of first-stage estimates from studies using wind direction as an instrument for pollution (Deryugina et al., 2019; Herrnstadt et al., 2021). The difference is that these studies use panel data to elicit short-run impacts. To demonstrate the advantage of our exposure measure for predicting pollution, we replicate the conventional wind instrument, aggregate to a cross-section, and estimate Equation 3 with this measure using pollution as an outcome. Appendix C provides more details of the replication.

Table B8 Panel A reports diagnostics for how the conventional measure fares against HYSPLIT for predicting NO_2. Column 1 shows the R^2 to assess explanatory power and the remaining two columns show F-statistics to assess predictive accuracy. Column 2 shows the the Kleibergen and Paap (KP) F-statistic, a heteroskedasticity-robust analog of the first stage F-statistic (Kleibergen and Paap, 2006). Column 3 shows the Olea and Pflueger (2013) F-statistic, an adjustment of KP statistic that accommodates panel data. Whereas both measures explain equal variation in NO_2 (column 1), HYSPLIT is a much stronger predictor of pollution than the conventional measure. The KP F-statistic for HYSPLIT (column 2, row 1) is twice as large as the standard measure. The gain remains equal under the adjusted F-statistic (column 3). For SO_2 (Panel B), both F-statistics are again larger for the HYSPLIT measure, although the gap is smaller compared to NO_2.

4.3 Heterogeneity: Health Effects are Less Pronounced in Urban Areas

The baseline findings describe average impacts *across districts*. This section investigates heterogeneity by urban form. Despite the conditional exogeneity of our exposure measure, we expect urban and rural districts to experience different health impacts from the same level of exposure. On one hand, population dense districts suffer worse population exposure due to sheer numbers. On the other, these are typically large cities with better health infrastructure, which dampens the health impact of pollution exposure compared to rural districts. It should be noted that power plant exposure itself does not directly affect local development (Table 6), rendering ex-post economic activity a suitable variable upon which to estimate heterogeneity.

Table 4 columns 1-3 present estimates from Equation 3 with an interaction for population density. Health effects are *less* pronounced in urban areas. Across all mortality indicators, additional deaths from cumulative exposure (first row) is 25% less in population dense districts compared to sparser ones (second row). The negative sign on population density (third row) suggests that

[8]Source apportionment studies show that coal power plants account for 7% of ambient $PM_{2.5}$ (Venkataraman et al., 2018) and between 30-50% of NO_2 and SO_2 (Lu and Streets, 2012; Lu et al., 2013).

Table 4: Heterogeneity by Urban Form

	Neonatal	Infant	Child	Neonatal	Infant	Child
	(1)	(2)	(3)	(4)	(5)	(6)
Capacity-weighted Exposure	1.116***	1.770***	2.219***	1.074***	1.725***	2.272***
	(0.314)	(0.476)	(0.585)	(0.342)	(0.531)	(0.649)
Capacity-weighted Exposure × Pop. Density	-0.277***	-0.457***	-0.555***			
	(0.078)	(0.122)	(0.151)			
Pop. Density	-0.170***	-0.278***	-0.337***			
	(0.042)	(0.066)	(0.082)			
Capacity-weighted Exposure × Nightlights				-0.097**	-0.162**	-0.213**
				(0.042)	(0.064)	(0.081)
Nightlights				-0.283***	-0.447***	-0.550***
				(0.034)	(0.055)	(0.070)
Controls	Yes	Yes	Yes	Yes	Yes	Yes
Outcome Mean	29.071	46.463	58.458	29.071	46.463	58.458
Exposure SD	25.140	25.140	25.140	25.140	25.140	25.140
State × Year FEs	✓	✓	✓	✓	✓	✓
Observations	1920	1920	1920	1920	1920	1920
Clustering	0.789	0.815	0.842	0.797	0.821	0.847

* $p < .1$, ** $p < .05$, *** $p < .01$. Data are district-yearly for 2000, 2007, and 2017. Mortality is measured per 1000 live births. SO_2 and NO_2 are in Dobson Units. $PM_{2.5}$ is in $\mu g/m^3$. Exposure is cumulative over 30 years, has a 50km mask, and standardized. District population density is from the 2011 census. Nightlight intensity is measured as luminosity values. Geography controls include: distance to nearest power plant, district area, water area within 25km, distance to nearest coal deposit, nearest coal area, elevation, slope, temperature and rainfall. Standard errors clustered by plume.

urban areas tend to be healthier. This corroborates the idea that an "urban advantage" protects the population from power plant exposure, likely through better health care access and quality.

The urban advantage is robust to other measures of population density. Columns 4-6 use nightlight intensity, a common proxy for population activity (Henderson et al., 2012), as the interaction term. The signs and significance of coefficients mirror column 1-3. Across all mortality measures, the mitigating effect of nightlights is about 10%.

4.4 Dynamics of Long Run Estimates

Our main finding is that districts historically exposed to coal power plant emissions experience worse present-day child mortality. Next, we investigate which specific periods of exposure are most important for determining current health outcomes. We then discuss how to interpret long run estimates and whether or not they are informative of short-run responses.

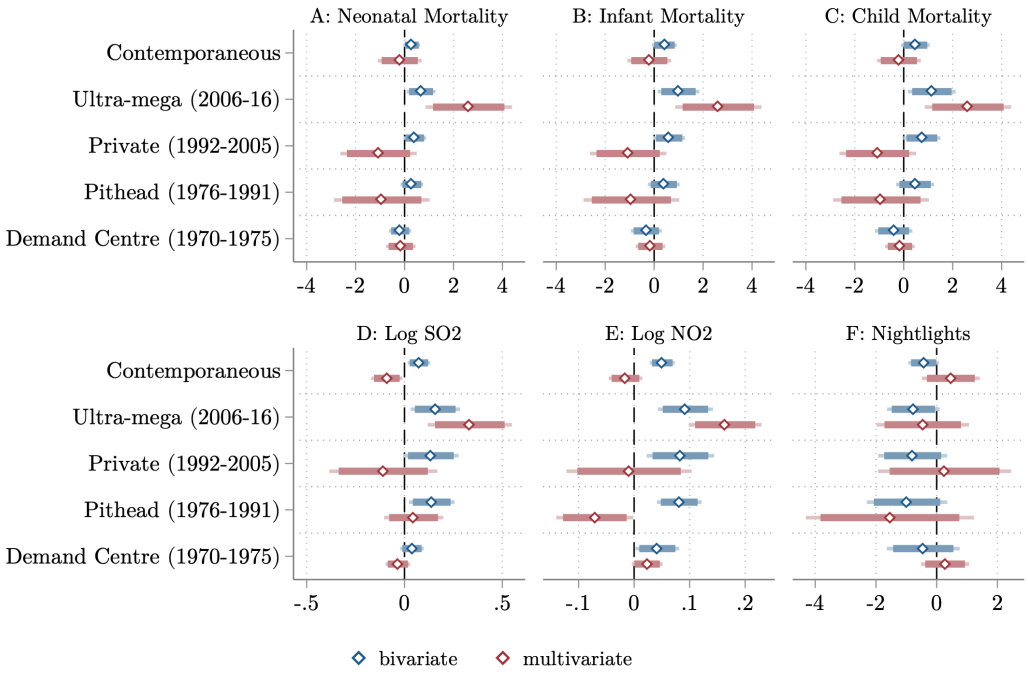

Figure 4: Dynamic Effects of Historic Coal Expansion Phases

Note: Outcome data are for 2017. Cumulative exposure covers each time bin (y-axis) and is divided by bin size. Bivariate coefficients and 95% confidence intervals (blue) are from five regressions of cumulative exposure during each time bin on the outcome with controls and state fixed-effects. The multivariate specification (red) shows coefficients from a single regression where exposure in each time bin is included in one equation. Exposure includes a 50km mask and is standardized. Controls include: distance to nearest power plant, district area, water area within 25km, distance to nearest coal deposit, nearest coal area, elevation, slope, temperature and rainfall. Standard errors clustered by plume.

4.4.1 Time Decomposition

Methods. To investigate when our estimates materialize, we unravel cumulative exposure into distinct time bins and then estimate Equation 3 as follows:

$$\begin{aligned} Mortality_{d(t=2017)} = \beta_1 CmlExposure_{d(t=2017)} + \beta_2 \sum_{t=2006}^{2016} CmlExposure_{dt} + \beta_3 \sum_{t=1992}^{2005} CmlExposure_{dt} \\ + \beta_4 \sum_{t=1976}^{1991} CmlExposure_{dt} + \beta_5 \sum_{t=1970}^{1975} CmlExposure_{dt} + \beta_6 \overline{X}_{dt} + \gamma_{st} + \epsilon_{dt} \end{aligned} \tag{6}$$

Bins span four periods marked by policy changes to the electricity sector, ranging from 1970-75, when small plants were sited near demand centres, to 2006-16, when the sector unbundled and ultra-mega power plants (4000+ MW) were rolled out (see Figure A3 for full timeline). A 2017 bin is included to capture the period of in-utero exposure. Cumulative exposure is divided by bin size for consistent coefficient interpretation. Fixed effects and controls are the same as Equation 3.

We estimate bivariate and mutivariate specifications. The bivariate case estimates dynamic effects as separate regressions, one for each time bin. Since other bins are excluded, short and

long run channels become bundled. For example, a positive coefficient on the 1970-75 bin need not represent pure long run effects. If plants are clustered together thereafter, then the coefficient also captures short run responses to exposure from plants built in the current period. In contrast, the multivariate case estimates dynamic effects with all time bins in one regression. Coefficients represent pure long term effects, *net* of short run responses or correlation with other periods.

Results: Dynamic Effects. Dynamic results are plotted in Figure 4. Blue and red denotes bivariate and multivariate cases, respectively. The first noteworthy result is that exposure to power plants in-utero and during the periods when privately (1992-2005) and ultra-mega plants (2006-16) were built have a positive and statistically significant impact on all mortality outcomes under the bivariate case (Panels A-C, blue). However, only the ultra-mega effect remains under the multivariate case (Panels A-C, red), suggesting that the bivariate effects were driven by persistence and the resulting response to short run exposure. Overall, this first result suggests that the pure long run impact of historic exposure on present-day mortality is driven by exposure to power plant emissions in the decade before child birth. Since contemporaneous exposure is a covariate in the multivariate (red) case, the mechanism must be through a channel *other than* in-utero exposure. We discuss candidate explanations in the next subsection.

The second result is that exposure to higher ambient pollution in the decade before child birth is the main mechanism underlying long run mortality impacts. In the bivariate case, exposure from 1976 onwards influences present day SO_2 and NO_2 levels (Panels D and E, blue). This implies that sites of past power plant construction influence current plant sites and, through this channel, influence current cross-sectional variation in pollution. Again, only the ultra-mega pollution effect remains positive under the multivariate case (Panels D and E, red). Overall, Panels A-E indicate that exposure to emissions during the decade before child birth influences early-life mortality through worse air quality arising from emissions during the same decade.

The third result is that the decomposition shows no effect when economic activity, measured by nightlight intensity, is the outcome (Panel F). This helps rule out adaptation as an alternative mechanism (we show this formally in section 4.6). If historic capacity expansions caused exposed districts to invest in adaptation more than non-exposed districts, then we would expect positive and significant coefficients. We would also expect no mortality differences, which is not the case.

4.4.2 Interpretation and Relation to Main Estimates

The contemporaneous bivariate coefficient in Panels A-C describe short run mortality impacts (Equivalent to Table B4, Section 4.1.3). An important question is: to what extent are our main long run estimates (Table 2) capturing these short run responses? Since marginal exposure may accumulate any time over the past three decades, it may reflect the short run effect if most accumulation occurs in the past year. Figure 4 helps answer this question since it tests the effect of marginal exposure accumulated at various time periods. If long run estimates were measuring short run responses, then all bins would become insignificant in the multivariate case since

Table 5: Robustness Checks: Neonatal Mortality

	(1)	(2)	(3)	(4)	(5)	(6)
Capacity-weighted Exposure	0.592** (0.256)	0.650*** (0.216)	0.650** (0.291)	0.650*** (0.245)	0.650*** (0.215)	1.993 (3.071)
Dataset	GBD	GBD	GBD	GBD	GBD	NFHS
Mask	None	50km	50km	50km	50km	50km
Plant Districts	No	Yes	Yes	Yes	Yes	Yes
Outcome Mean	29.224	29.071	29.071	29.071	29.071	29.752
Exposure SD	23.960	25.140	25.140	25.140	25.140	23.572
State FEs						✓
State × Year FEs	✓	✓	✓	✓	✓	
Clustering	Plume	Plume (50)	Conley (100)	Conley (200)	Conley (500)	Plume
Observations	1678	1920	1920	1920	1920	526

* $p < .1$, ** $p < .05$, *** $p < .01$. Column 1 omits power plant districts. Column 2 uses k-means to define 50 plumes and clusters error by plume. Columns 3-5 show Conley standard errors for different kernel cutoff distances (in km). Column 6 uses data from the NFHS-IV survey. All columns control for: distance to nearest power plant, district area, water area within 25km, distance to nearest coal deposit, nearest coal area, elevation, slope, temperature and rainfall.

short run responses are controlled for. The fact that the coefficient on the 2006-16 bin remains positive and significant suggests that the short and long run impacts of power plant exposure on present-day health are measuring two very different types of responses.

Short run estimates reflect early-life mortality impacts of in-utero exposure to emissions, a well documented phenomenon (Currie and Neidell, 2005; Von der Goltz and Barnwal, 2019). In contrast, long run multivariate estimates reflect mortality impacts through another channel, most likely institutional determinants of health. For example, exposure to power plant emissions in the decade before child birth can affect maternal health, well-being, and other socioeconomic characteristics that translate into lower chance of child survival (Perera and Herbstman, 2011).

4.5 Robustness: Sensitivity Tests

This section presents additional robustness tests to establish confidence in our mortality estimates. These include sample restrictions, alternative standard error clustering, and estimates from an alternative dataset. Robustness tables are shown for neonatal mortality (Table 5). The same tables for infant and child mortality are in Appendix B6 and B7.

Dropping Power Plant Districts. Whereas the main results (Table 2) showed that estimates are stable under varying masks, column 1 tests robustness to dropping power plant districts altogether. This leaves coefficients to be identified off of plausibly random wind-driven emissions exposure rather than potentially endogenous placement-driven exposure. The neonatal mortality estimate is very similar to the main estimates with mask size 5-50km.

Alternative Clustering. Standard errors are clustered by plume throughout the paper, with 25 plumes demarcated through a k-means algorithm. Column 2 shows that standard errors are stable when 50 plumes are demarcated instead. Columns 3-5 investigate spatial clustering more

Table 6: Adaptation to Long Term Power Plant Exposure

	Adaptation			Sorting	
	(1) Consumption	(2) Services	(3) Nightlights	(4) Immigration	(5) Immigration
Capacity-weighted Exposure	-220.005* (121.957)	0.059 (0.039)	0.068 (0.059)	-0.358 (0.223)	0.005 (0.003)
Controls	Yes	Yes	Yes	Yes	Yes
Data Source	SECC	EC	DMSP	Census D3	IHDS
Year	2012	2013	2013	2011	2012
Outcome Mean	17885.797	0.756	10.479	5.202	0.098
Exposure SD	25.888	27.787	27.846	24.405	36.154
State FEs	✓	✓	✓	✓	✓
Clustering	Plume	Plume	Plume	Plume	Plume
N	615	615	611	628	36731
R^2	0.709	0.690	0.729	0.659	0.031

* $p < .1$, ** $p < .05$, *** $p < .01$. Note: Each column is a cross-sectional regression from various data sources and years (see footer). The outcome in column 1 is mean per capita consumption. Column 2 is log employment in the service sector plus 1. Column 3 is log light intensity across district pixels. Column 4 is the district population share of migrants who moved with their families in the past 30 years. Column 5 is a household indicator for entire-family migration from the IHDS-II survey. Exposure is cumulative over 30 years, includes a 50km mask, and standardized. All columns control for: distance to nearest power plant, district area, water area within 25km, distance to nearest coal deposit, nearest coal area, elevation, slope, temperature and rainfall. Standard errors clustered by plume level.

systematically by implementing Conley (1999) standard errors. Reassuringly, precision remains stable even when allowing for long distance spatial error correlation up to 500km.

Estimates from NFHS Survey. Column 6 presents estimates with mortality computed from the 2015-16 NFHS demographic survey. This survey is among the various raw sources contributing to the main GBD mortality data used throughout the paper (section 2.1). The NHFS survey covers 600,000 households across 29 states and is representative at the district level. Eligible women report survival and age at death for all births. We compute district mortality rates using 2015 birth histories, a year during which recall bias is minimal, and then replicate Equation 3.

The neonatal mortality effect remains positive but precision is lowered (column 6). However, note that precision is also weak in the 2017 cross-section of the main analysis (column 7 table B3), the closest comparison period. We posited that pollution reduction from offlining vintage plants can explain the imprecision (Figure A2).

Robustness of Infant and Child Mortality. Tables B6 and B7 show the same robustness checks for infant and child mortality, respectively. Estimates remain stable across all specifications. Similar to the neonatal mortality case (Table 5), the coefficient remains positive but precision is low when the main equation is estimated on the NFHS survey (column 7).

4.6 Robustness: Adaptation and Sorting

This section investigates and rules out adaptation and residential sorting as alternative mechanisms for our main results.

Differential Development. Figure 4D showed that emissions exposure during various historic periods had no persistent effects on economic activity. We corroborate this formally with additional measures of economic development from the SHRUG database (Section 2.1). We replicate Equation 3 for the year in which each development indicator is provided.

There is little evidence of adaptation (Table 6). Districts exposed to power plant emissions in the long run have weakly lower consumption per capita (column 1), no difference in service sector employment (column 2), and no difference in economic activity (column 3) compared to less-exposed districts in the same state. The economic significance of the consumption effect (column 1) is negligible as it reflects only 1% of the mean. These findings bolster our claim that long run effects of power plant exposure on health operate through pollution, not adaptation.

Selective Migration. Residential sorting is another competing explanation for our results. If healthy people move to less-exposed areas, then control districts are contaminated and mortality estimates are inflated. Coefficients would reflect sorting and not the causal health impact of long run exposure to power plants. Indeed, Heblich et al. (2016) show path-dependent sorting following power plant exposure in 19th century England. This is not expected in India due to socioeconomic mobility barriers and historically low migration (Munshi and Rosenzweig, 2016).

We formally test for residential sorting using two high-quality data sources. First, the recently released migration module of the 2011 Census, from which we compute the district immigrant share having arrived with their whole family from another district in the past 30 years. Second, the 2012 round of the India Human Development Survey (IHDS), which is representative at the state level, covers 40,000 households and asks if and when they moved to the current district. We leave data at the household level and construct an indicator for whether the household moved to their current residence with their whole family within the past 30 years.

We use the Census immigrant share and IHDS relocation indicator as outcomes in Equation 3 to test for sorting. If exposure "pushes" families into cleaner districts, then $\beta_1 < 0$ (less migration into dirty districts compared to clean ones). Columns 5 and 6 of Table 6 show no evidence of selective migration at the district or household level, respectively. This suggests that historic exposure does not trigger path-dependent sorting and helps rule out endogenous migration as an alternative explanation for our main estimates. These results also bolster our claim that pollution is the key mechanism driving health disparities between exposed and non-exposed districts.

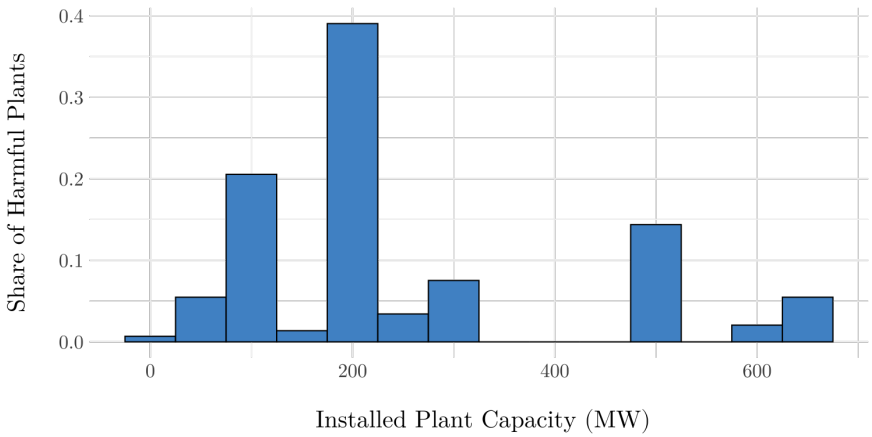

Figure 5: Distribution of installed capacity among harmful plants

Note: Histogram of installed capacity (MW) among harmful plants. Harmful plants are those that significantly increase mortality in the plant-level regressions of mortality on cumulative exposure (Equation 7).

5 Policy Analysis

Having quantified the death rate from long run exposure to power plant emissions, this final section turns to an investigation of how energy policy can minimize these impacts. We first identify which power plants drive the mortality effects. We then aggregate our district-level estimates to study avoided deaths at the national level under various abatement scenarios.

5.1 Which power plants are responsible?

Methods. In Equations 1 and 2 particle counts are summed over all power plants j and districts d to compute districts' cumulative exposure to all plants. Here, we leave gridded particle counts at the plant level and then aggregate cumulative exposure to each plant j at the district level. We then estimate the main equation 565 times, once for each plant:

$$Mortality_{dt} = \beta_1 CmlExposure_{jdt} + \beta_2 \overline{X}_{dt} + \gamma_{st} + \epsilon_{jdt}, \tag{7}$$

where $CmlExposure_{jdt}$ is cumulative exposure of district d to power plant j at time t. All other terms are the same as Equation 3. We then collect plant identifiers for which β_1 is positive and significant. We call these "harmful" plants. Lastly, we characterize these harmful plants based on the limited information (location and size) we have about them from the CEA dataset.

Characterization of Harmful Plants. Based on this method, the mortality effects in the main analysis are driven by 146 plants (out of 565). Figure A4 shows their location: although scattered across the country, many are clustered in Eastern India near the coal belt. These reflect older, inefficient plants built during the coal-by-wire policy period.

Figure 5 plots the distribution of installed capacity among harmful plants. The majority are

200 MW, which is within the size bandwidth defined by the International Energy Agency as "sub-critical". These plants are considered inefficient and require more fuel to generate the same amount of power as higher capacity plants, creating more pollution in the process. Figure A5 shows the plant size distribution by decade of construction. Most harmful plants were commissioned during the 1970s, 80s, and 90s. During the 2000s, when larger plants became more common, higher capacity plants overtake sub-critical ones in terms of driving mortality effects.

Policy Implications. Our plant-level estimates suggest that sub-critical plants drive power plant emissions-related deaths. Nearly 90% of these are government owned (Caldecott et al., 2015). After the Paris Agreement, India revised its National Electricity Plan to decommission 25+ year old plants (Ministry of Power, 2018). However, this plan was reversed several years later, citing surges in electricity demand (Varadhan, 2023). Although the phase-down was originally pledged to meet climate targets, our analysis shows that the phase-down would also deliver dramatic health benefits. In the next section we quantify these benefits in terms of avoided deaths.

5.2 Counterfactual simulations under alternative abatement scenarios.

Methods. HYSPLIT emissions trajectories are generated *for each plant* before scaling by installed capacity and aggregating over districts (Section 2.2). This allows us to easily change underlying capacity weights or delete plants altogether to simulate district-level exposure under alternative scenarios. Consider two scenarios for simulation: first, India complies with its Paris Pledge, where it committed to 50% of installed capacity from renewable energy by 2030 (Government of India, 2022). Assuming the remaining grid is coal powered, this requires reducing coal-fired installed capacity by about 25%[9]. In the second scenario, India shuts down plants operating for 25+ years.

For each district d, we use the regression model from Equation 3 to predict neonatal mortality rates ($NNMR_d$) in 2017 under each scenario:

$$NNMR_d^{Paris} = \hat{\beta_1} CmlExposure_d^{Paris} + \hat{\beta_2}\overline{X}_d + \gamma_s + \mu_d$$

$$NNMR_d^{Retire} = \hat{\beta_1} CmlExposure_d^{Retire} + \hat{\beta_2}\overline{X}_d + \gamma_s + \mu_d$$

where $CmlExposure_d^{Paris}$ denotes realizations of cumulative emissions exposure when the underlying installed capacity of each plant is reduced by 25%. $CmlExposure_d^{Retire}$ leaves plant capacity unchanged but drops plants commissioned before 1992. We multiply predicted mortality by the number of live births in each district[10] to enable aggregation of local predictions into national counterfactuals, $NatNND^{Paris}$ and $NatNND^{Retire}$. These measure total neonatal deaths if India met its Paris pledge and if it retired vintage plants, respectively. Comparison with in-sample fit-

[9] At the end of our study period, total installed capacity from thermal and renewable sources was 320,052 MW with each source making up 68% and 32%, respectively (Central Electricity Authority, 2020a) [Table 2]. Assuming no grid expansion until 2030, bringing installed coal capacity to the Paris Pledge level (0.5*320,052 MW = 160,026 MW) from its current level (0.68*320,052 MW = 217,635 MW) involves a 26% reduction.

[10] Data are obtained from India's Central Registration System

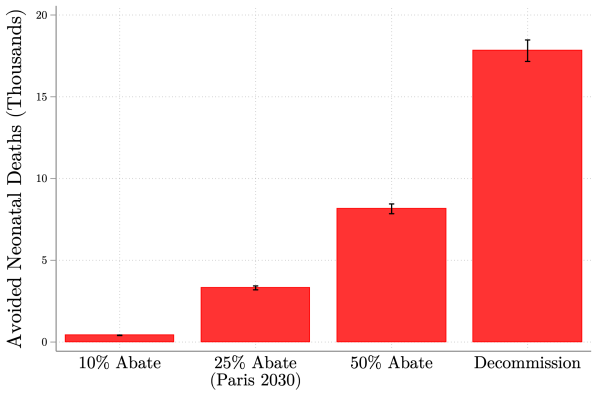

Figure 6: Total Avoided Deaths Under Abatement Scenarios

Note: y-axis is total number of neonatal deaths avoided under each scenario (Equation 8). Under the 10%, 25% and 50% scenarios, plant capacity is reduced by these amounts before weighting and aggregating (section 2.2). Under the decommission scenario, 25+ year old plants are removed. Confidence intervals computed from 1000 bootstrap draws.

ted values $NatNND$ (the status quo) yields the main statistic of interest, avoided deaths under each scenario:

$$\begin{aligned} AvoidedDeaths^{Paris} &= NatNND^{Paris} - NatNND \\ AvoidedDeaths^{Retire} &= NatNND^{Retire} - NatNND \end{aligned} \tag{8}$$

Beyond these, we compute avoided deaths under 10% and 50% capacity reduction scenarios.

Simulation Results. Figure 6 reports our estimates of avoided deaths under each abatement scenario (Equation 8). Error bars correspond to 95% confidence intervals from bootstrapping the prediction and aggregation procedure with 1000 draws. 3,300 neonatal deaths could be avoided if India met its Paris Pledge. If it retired vintage power plants, the number of avoided deaths would increase nearly six times compared to the Paris scenario. It is important to note that these are long term simulations i.e., if India decomissioned old power plants today, 18,000 neonatal deaths would be avoided due to lower emissions exposure *over the next three decades*.

Figure 7 illustrates the spatial distribution of avoided deaths across districts. Values are computed by estimating Equation 8 on non-aggregated predictions under each scenario. In all scenarios, benefits from abatement are largely concentrated in eastern India. This is somewhat unsurprising given that many of these districts are near highly emitting plant clusters in the coal belt (Figure 2A). Importantly, avoided deaths are clearly observed in parts of South India, especially, where power plants are sparse. These regions experience positive spatial spillovers from plant capacity reductions elsewhere.

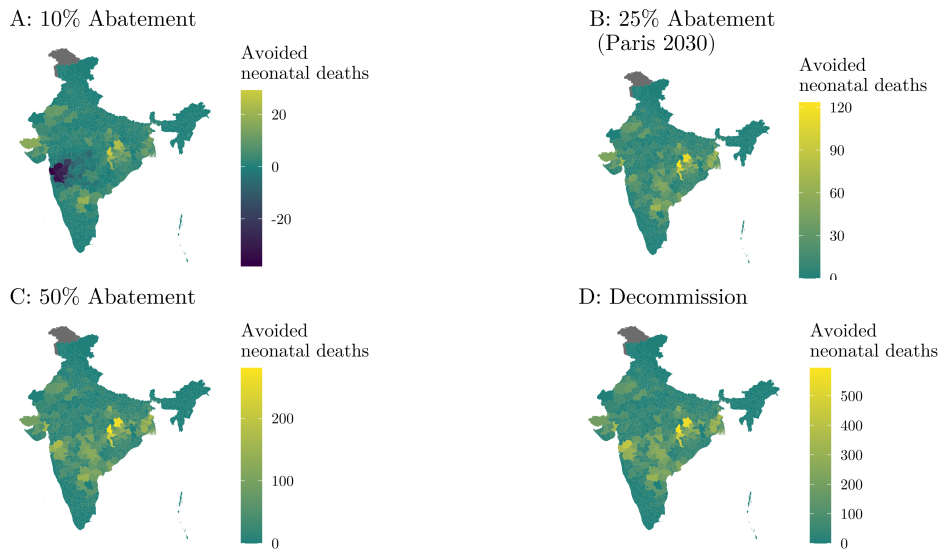

Figure 7: Avoided Deaths in Districts Under Abatement Scenarios

Note: Districts are colored by total neonatal deaths avoided (Equation 8 at the district level). Under the 10%, 25% and 50% scenarios, plant capacity is reduced by these amounts before weighting and aggregating (section 2.2). Under the decommission scenario, 25+ year old plants are removed. Values represent means over 1000 bootstrap draws.

6 Conclusion

Coal is being phased out of the energy system across the developed world, yet remains a dominant fuel in many developing countries. In India, coal-fired power plants generated 63% of electricity in 2016 (Shearer et al., 2017). The equivalent share in China is 60%. Although electricity access delivers salient economic benefits, this paper focuses on costs. Until now, previous studies documented short run negative health effects from exposure to coal power plants using monthly or annual panel data. We extend this literature by documenting novel evidence on the impact of long run exposure to coal-fired power plant emissions in India over three decades.

We find that districts historically exposed to higher power plant emissions experience worse present-day neonatal, infant, and child mortality rates. To establish this, we develop a novel measure of historic emissions exposure from an atmospheric dispersion model that draws wind-driven particle trajectories from every power plant in India. We also verify that our mortality estimates are driven by higher local pollution and not through differential adaptation or residential sorting. Lastly, we unravel historic exposure and find that present-day mortality is most sensitive to exposure during the 2006-16 era, the period during ultra-mega power plants were rolled out.

Our results imply that there is ample room for energy policy to minimize health impacts. Our plant-level analysis reveals that inefficient, older plants drive the bulk of mortality effects. Our counterfactual simulations show that offlining these vintage plants can avoid 18,000 neonatal deaths in the long run. This amounts to approximately $USD 5.6 billion in savings using the value of a statistical life for India (Gulati et al., 2021)[11].

[11] Gulati et al. (2021) estimate a VSL of $USD 312,663 for India in 2013. Details in the Methods section of their paper.

A Appendix Figures

Figure A1: Plume Clusters (n=25)

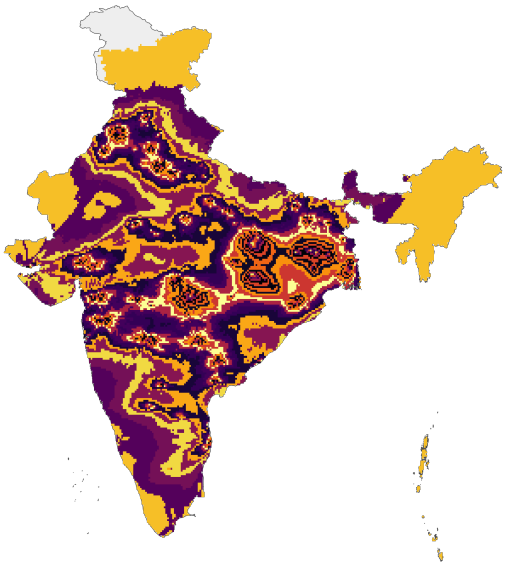

Note: Colours represent 25 clusters of cells grouped together according to a k-means algorithm. These clusters are used for clustering standard errors in the main analysis.

Figure A2: Event Study: Number of Years Power Plant Active in District

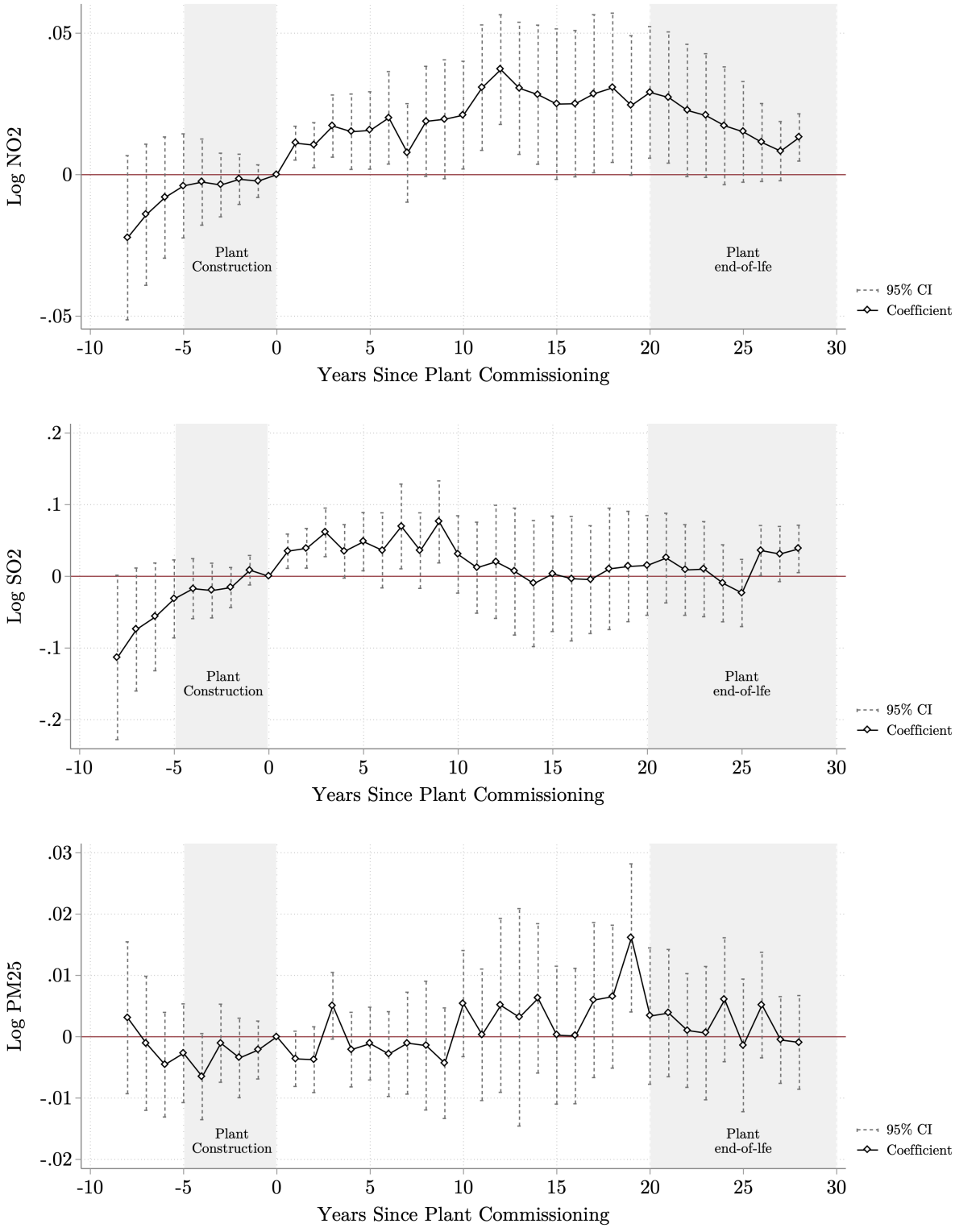

Note: white diamonds are coefficients from an event study regression at the plant level (Equation 5). x-axis is number of years the plant has been active in a district. Year of plant commissioning is normalized to zero. Dotted lines are 95% confidence intervals. All regressions include plant and state-year fixed effects as well as controls for installed capacity, temperature, and rainfall. Standard errors clustered at the district level.

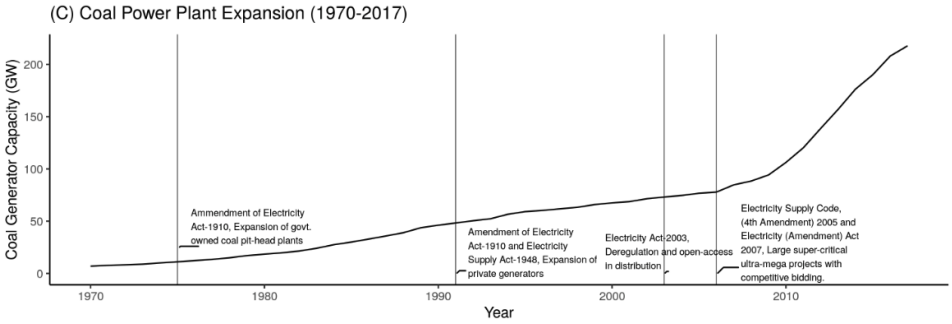

Figure A3: Timeline of Coal Power Plant Capacity Expansion

Total installed capacity from 1970-2017. Vertical lines denote important policy changes to the electricity sector.

Figure A4: Location of Harmful Plants

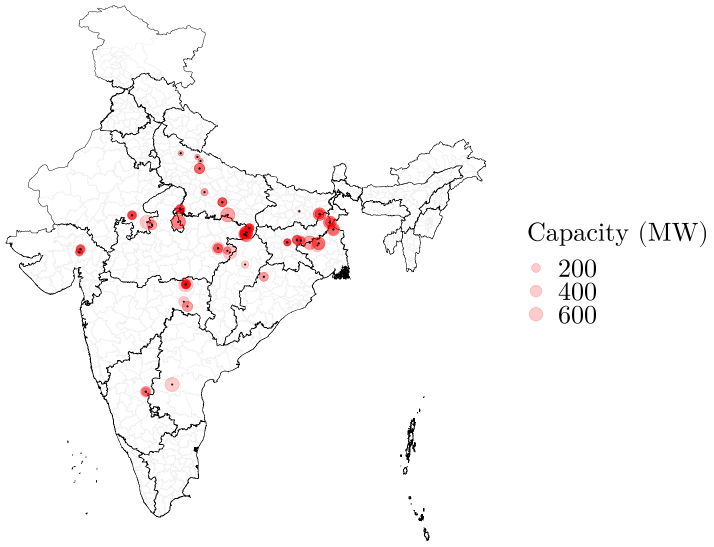

Note: Black dots indicate location of power plants with positive and significant effect on neonatal mortality from plant-level regressions (Equation 7). Red circles vary with plant size (MW).

Figure A5: Size of Harmful Plants by Decade of Construction

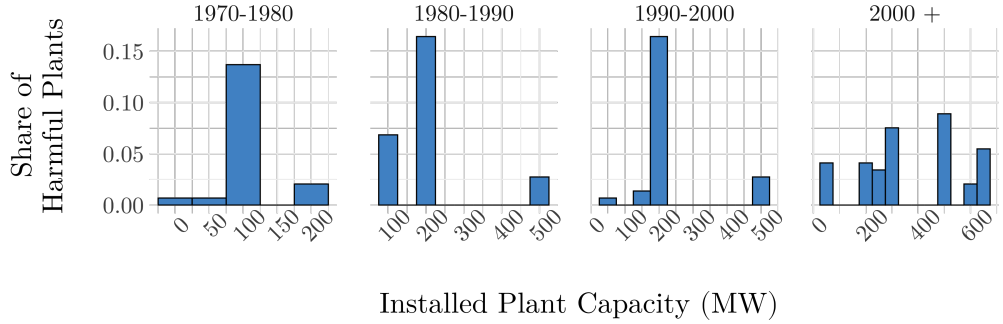

Note: Histogram of plant size among harmful plants by decade of construction. Harmful plants are those that significantly increase mortality in the plant-level regressions of mortality on exposure (Equation 7).

B Appendix Tables

Table B1: Long Term Impact of Historic Exposure on Infant Mortality

	(1)	(2)	(3)	(4)	(5)	(6)
Capacity-weighted Exposure	0.357*	0.632***	0.734***	0.764***	0.902***	0.997***
	(0.198)	(0.202)	(0.227)	(0.243)	(0.302)	(0.325)
Nearest Plant	Yes	Yes	Yes	Yes	Yes	Yes
Geography Controls	No	Yes	Yes	Yes	Yes	Yes
Mask	None	None	5km	10km	30km	50km
Outcome Mean	46.463	46.463	46.463	46.463	46.463	46.463
Exposure SD	39.517	39.517	36.039	34.370	29.388	25.140
State × Year FEs	✓	✓	✓	✓	✓	✓
Observations	1920	1920	1920	1920	1920	1920
R^2	0.801	0.810	0.810	0.811	0.811	0.811

* $p < .1$, ** $p < .05$, *** $p < .01$. Data are district-year level for 2000, 2007, and 2017. Mortality measured per 1000 live births. Exposure is cumulative over 30 years and standardized. Geography controls include: distance to nearest plant, district area, water area within 25km, distance to nearest coal deposit, nearest coal area, elevation, slope, temperature and rainfall. Mask is radius within which exposure gridcells are deleted. Standard errors clustered by plume.

Table B2: Long Term Impact of Historic Exposure on Child Mortality

	(1)	(2)	(3)	(4)	(5)	(6)
Capacity-weighted Exposure	0.498**	0.856***	0.981***	1.012***	1.173***	1.278***
	(0.244)	(0.251)	(0.287)	(0.308)	(0.385)	(0.411)
Nearest Plant	Yes	Yes	Yes	Yes	Yes	Yes
Geography Controls	No	Yes	Yes	Yes	Yes	Yes
Mask	None	None	5km	10km	30km	50km
Outcome Mean	58.458	58.458	58.458	58.458	58.458	58.458
Exposure SD	39.517	39.517	36.039	34.370	29.388	25.140
State × Year FEs	✓	✓	✓	✓	✓	✓
Observations	1920	1920	1920	1920	1920	1920
R^2	0.831	0.838	0.839	0.839	0.839	0.839

* $p < .1$, ** $p < .05$, *** $p < .01$. Data are district-year level for 2000, 2007, and 2017. Mortality measured per 1000 live births. Exposure is cumulative over 30 years and standardized. Geography controls include: distance to nearest plant, district area, water area within 25km, distance to nearest coal deposit, nearest coal area, elevation, slope, temperature and rainfall. Mask is radius within which exposure gridcells are deleted. Standard errors clustered by plume.

Table B3: Cross-sectional Long Term Impact of Historic Exposure on Mortality

	2000			2007			2017		
	(1) Neonatal	(2) Infant	(3) Child	(4) Neonatal	(5) Infant	(6) Child	(7) Neonatal	(8) Infant	(9) Child
Capacity-weighted Exposure	1.166** (0.458)	1.973** (0.703)	2.856*** (0.913)	1.015** (0.448)	1.568** (0.683)	1.973** (0.801)	0.443** (0.212)	0.650** (0.301)	0.759** (0.344)
Controls	Yes	Yes	Yes	Yes	Yes	Yes	Yes	Yes	Yes
Outcome Mean	36.254	59.880	78.700	28.496	45.182	55.810	22.462	34.326	40.865
Exposure SD	12.571	12.571	12.571	19.585	19.585	19.585	35.365	35.365	35.365
State FEs	✓	✓	✓	✓	✓	✓	✓	✓	✓
Observations	640	640	640	640	640	640	640	640	640
R^2	0.723	0.737	0.772	0.704	0.727	0.746	0.711	0.737	0.745

* $p < .1$, ** $p < .05$, *** $p < .01$. Data are district-year level for 2000, 2007, and 2017. Mortality measured per 1000 live births. Exposure is cumulative over 30 years and standardized. Geography controls include: distance to nearest plant, district area, water area within 25km, distance to nearest coal deposit, nearest coal area, elevation, slope, temperature and rainfall. Mask is radius within which exposure gridcells are deleted. Standard errors clustered by plume.

Table B4: Cross-sectional Short Term Impact of Historic Exposure on Mortality

	2000			2007			2017		
	(1) Neonatal	(2) Infant	(3) Child	(4) Neonatal	(5) Infant	(6) Child	(7) Neonatal	(8) Infant	(9) Child
Capacity-weighted Exposure (Short Term)	2.400** (0.873)	4.178*** (1.430)	5.910*** (1.900)	2.691*** (0.743)	4.197*** (1.201)	5.388*** (1.466)	0.478** (0.195)	0.696** (0.283)	0.786** (0.323)
Controls	Yes	Yes	Yes	Yes	Yes	Yes	Yes	Yes	Yes
Outcome Mean	36.254	59.880	78.700	28.496	45.182	55.810	22.462	34.326	40.865
Exposure SD	0.945	0.945	0.945	1.101	1.101	1.101	4.620	4.620	4.620
State FEs	✓	✓	✓	✓	✓	✓	✓	✓	✓
Observations	640	640	640	640	640	640	640	640	640
R^2	0.724	0.738	0.773	0.706	0.729	0.748	0.712	0.738	0.746

* $p < .1$, ** $p < .05$, *** $p < .01$. Data are district-year level for 2000, 2007, and 2017. Mortality measured per 1000 live births. Short-term exposure is cumulative exposure in year t minus $t-1$. Exposure includes a 50km mask and is standardized. Geography controls include: distance to nearest power plant, district area, water area within 25km, distance to nearest coal deposit, nearest coal area, a coastal indicator, elevation, slope, temperature and rainfall. Standard errors clustered by plume.

Table B5: Cross-sectional Impact of Historic Exposure on Log Pollution

	2000			2007			2017		
	(1) SO2	(2) NO2	(3) PM2.5	(4) SO2	(5) NO2	(6) PM2.5	(7) SO2	(8) NO2	(9) PM2.5
Capacity-weighted Exposure	0.265** (0.107)	0.119*** (0.030)	-0.024 (0.016)	0.164** (0.073)	0.083*** (0.018)	0.004 (0.011)	0.116** (0.052)	0.070*** (0.022)	0.009 (0.010)
Controls	Yes	Yes	Yes	Yes	Yes	Yes	Yes	Yes	Yes
Exposure SD	12.571	12.571	12.571	19.585	19.585	19.585	35.365	35.365	35.365
State FEs	✓	✓	✓	✓	✓	✓	✓	✓	✓
Observations	640	640	640	640	640	640	640	640	640
R^2	0.526	0.856	0.887	0.541	0.856	0.896	0.617	0.843	0.914

* $p < .1$, ** $p < .05$, *** $p < .01$. Data are at the district-annual level for 2000, 2007, and 2017. SO_2 and NO_2 are measured in Dobson Units. $PM_{2.5}$ is measured in $\mu g/m^3$. Exposure is cumulative over 30 years, includes a 50km mask, and standardized. All specifications include controls for: distance to nearest power plant, district area, water area within 25km, distance to nearest coal deposit, nearest coal area, a coastal indicator, elevation, slope, temperature and rainfall. Standard errors clustered at the plume level.

Table B6: Robustness Checks: Infant Mortality

	(1)	(2)	(3)	(4)	(5)	(6)
Capacity-weighted	0.880**	0.997***	0.997**	0.997***	0.997***	2.195
Exposure	(0.369)	(0.326)	(0.443)	(0.351)	(0.310)	(3.471)
Dataset	GBD	GBD	GBD	GBD	GBD	NFHS
Mask	None	50km	50km	50km	50km	50km
Plant Districts	No	Yes	Yes	Yes	Yes	Yes
Outcome Mean	46.845	46.463	46.463	46.463	46.463	38.448
Exposure SD	23.960	25.140	25.140	25.140	25.140	23.572
State FEs						✓
State × Year FEs	✓	✓	✓	✓	✓	
Clustering	Plume	Plume (50)	Conley (100)	Conley (200)	Conley (500)	Plume
Observations	1678	1920	1920	1920	1920	526

* $p < .1$, ** $p < .05$, *** $p < .01$. Note: Mask refers to a radius around each plant within which cell values are omitted. Column 2 omits districts with the power plant. Column 3 uses a 30km mask. Column 4 uses k-means clustering to define 50 plumes and clusters errors at this level. Column 5 unions cells in the 95th percentile of exposure values and clusters at this level. Column 6 uses data from the NFHS-IV survey. All specifications include controls for: distance to nearest power plant, district area, water area within 25km, distance to nearest coal deposit, nearest coal area, a coastal indicator, elevation, slope, temperature and rainfall. Standard errors clustered at the plume level with 25 plumes unless otherwise specified.

Table B7: Robustness Checks: Child Mortality

	(1)	(2)	(3)	(4)	(5)	(6)
Capacity-weighted	1.206**	1.278***	1.278**	1.278***	1.278***	2.089
Exposure	(0.485)	(0.401)	(0.534)	(0.421)	(0.400)	(3.487)
Dataset	GBD	GBD	GBD	GBD	GBD	NFHS
Mask	None	50km	50km	50km	50km	50km
Plant Districts	No	Yes	Yes	Yes	Yes	Yes
Outcome Mean	59.101	58.458	58.458	58.458	58.458	38.662
Exposure SD	23.960	25.140	25.140	25.140	25.140	23.572
State FEs						✓
State × Year FEs	✓	✓	✓	✓	✓	
Clustering	Plume	Plume (50)	Conley (100)	Conley (200)	Conley (500)	Plume
Observations	1678	1920	1920	1920	1920	526

* $p < .1$, ** $p < .05$, *** $p < .01$. Note: Mask refers to a radius around each plant within which cell values are omitted. Column 2 omits districts with the power plant. Column 3 uses a 30km mask. Column 4 uses k-means clustering to define 50 plumes and clusters errors at this level. Column 5 unions cells in the 95th percentile of exposure values and clusters at this level. Column 6 uses data from the NFHS-IV survey. All specifications include controls for: distance to nearest power plant, district area, water area within 25km, distance to nearest coal deposit, nearest coal area, a coastal indicator, elevation, slope, temperature and rainfall. Standard errors clustered at the plume level with 25 plumes unless otherwise specified.

Table B8: Comparison of Predictive Accuracy between HYSPLIT exposure and Wind Instrument

	Within R-sq.	F-Statistics	
		Kleibergen and Paap (2006)	Montiel Olea and Pflueger (2013)
	(1)	(2)	(3)
Panel A: Outcome: Log(NO2)			
Capacity-weighted Exposure (HYSPLIT)	0.55	32.80	28.90
Capacity-weighted Cone (Literature)	0.54	13.92	15.89
Panel B: Outcome: Log(SO2)			
Capacity-weighted Exposure (HYSPLIT)	0.19	12.06	11.00
Capacity-weighted Cone (Literature)	0.22	9.01	9.45

Note: each row shows model statistics from a regression of log pollution on cumulative exposure. Panel A uses log(NO2) as the outcome and Panel B uses log(SO2). Exposure is measured by HYSPLIT (Equation 1) or by replicating the conventional wind direction instrument from the literature and aggregating to 2000, 2007, and 2017 cross sections for consistency. Accumulation windows start from 1990 for both measures. All regressions include state-year fixed effects and controls for distance to nearest power plant, district area, water area within 25km, distance to nearest coal deposit, nearest coal area, elevation, slope, temperature and rainfall. HYSPLIT regressions clustered by plume and replication regressions by state.

C Replication of Wind Instrument and Comparison with HYSPLIT

This Appendix demonstrates the advantage of our exposure measure by comparing how accurately it predicts pollution compared to the standard wind direction measure from the literature.

Data Construction. Replication data for the wind direction measure consists of monthly gridded wind direction from 1990-2017 at $0.1 \times 0.1^{\circ}$ resolution[12]. First, we extract wind direction at each power plant pixel. Second, we define the exposure area as a 100km radius quarter-circle centered on the vector. Third, we distribute plant capacity over districts spanned by the cone, weighted by overlap fraction, and then sum over plants. Lastly, we accumulate the capacity-weighted cones from 1990 to produce a long run exposure measure that loosely resembles our measure. However, the lack of a dispersion model necessitates strict assumptions about plume shape and diffusion.

Estimation. After generating the cumulative version of the conventional wind-direction instrument, we extract three cross-sections from 2000, 2007, and 2017, the same years as our main data. Since the replication data starts in 1990, each cross-section has a 10 year accumulation window. We also adjust the accumulation window of $CmlExposure_{dt}$ down to 10 years for consistency. Finally, we estimate the below equation with log NO2 and SO2 as the outcome:

$$log(Pollution)_{dt} = \beta_1 CmlWindDirection_{dt} + \beta_2 \overline{X}_{dt} + \gamma_{st} + \epsilon_{dt} \tag{9}$$

where $Pollution_{dt}$ is ambient SO2 or NO2 concentration in district d during year $t \in \{2000, 2007, 2017\}$. $CmlWindDirection_{dt}$ is cumulative, wind-driven exposure in the past decade ($t-10$ and t) constructed using the literature (cone-based) method. $\overline{X}_{dt}$ is a covariate vector of site suitability met-

[12]We use the ERA5-Land monthly averaged data obtained from the Copernicus Climate Change Service

rics that account for the endogeneity of plant placement. State-year fixed effects, γ_{st}, ensure that cross-district comparisons are made within states separately in each of the three periods.

Tables B8 presents R^2 and F-statistics for Equation 9 and the same regression using $CmlExposure_{dt}$ from HYSPLIT. These diagnostics describe any gains in predictive strength of the HYSPLIT-generated exposure measure for predicting pollutuon compared to the standard literature measure. See main text (Section 4.2) for description of results.

References

Anderson, Michael L, "As the Wind Blows: The Effects of Long-Term Exposure to Air Pollution on Mortality," *Journal of the European Economic Association*, 10 2019, *18* (4), 1886–1927.

Arceo, Eva, Rema Hanna, and Paulina Oliva, "Does the effect of pollution on infant mortality differ between developing and developed countries? Evidence from Mexico City," *The Economic Journal*, 2016, *126* (591), 257–280.

Asher, Sam, Tobias Lunt, Ryu Matsuura, and Paul Novosad, "Development research at high geographic resolution: an analysis of night-lights, firms, and poverty in India using the shrug open data platform," *The World Bank Economic Review*, 2021, *35* (4), 845–871.

Barrows, Geoffrey, Teevrat Garg, and Akshaya Jha, "The Health Costs of Coal-Fired Power Plants in India," *IZA DP No. 12838*, 2019.

Blakeslee, David, Ram Fishman, and Veena Srinivasan, "Way down in the hole: Adaptation to long-term water loss in rural India," *American Economic Review*, 2020, *110* (1), 200–224.

Caldecott, Ben, Gerard Dericks, and James Mitchell, *Stranded assets and subcritical coal: the risk to companies and investors*, Smith School of Enterprise and the Environment, 2015.

Central Electricity Authority, "Review of Land Requirement for Thermal Power Stations," Technical Report 2010.

_ , "Report on Minimisation of Water Requirement in Coal Based Thermal Power Stations," Technical Report, Central Electricity Authority, New Delhi January 2012.

_ , "GROWTH OF ELECTRICITY SECTOR IN INDIA FROM 1947-2020," Technical Report 2020.

_ , "A Note on Retirement of 25 years or more old Coal / Lignite based Thermal Power Units," Technical Report 2020.

Chay, Kenneth Y and Michael Greenstone, "The impact of air pollution on infant mortality: evidence from geographic variation in pollution shocks induced by a recession," *The quarterly journal of economics*, 2003, *118* (3), 1121–1167.

Clay, Karen, Joshua Lewis, and Edson Severnini, "Canary in a Coal Mine: Infant Mortality, Property Values, and Tradeoffs Associated with Mid-20th Century Air Pollution," Working Paper 22155, National Bureau of Economic Research April 2016.

Conley, Timothy G, "GMM estimation with cross sectional dependence," *Journal of econometrics*, 1999, *92* (1), 1–45.

Cropper, Maureen, Ryna Cui, Sarath Guttikunda, Nate Hultman, Puja Jawahar, Yongjoon Park, Xinlu Yao, and Xiao-Peng Song, "The mortality impacts of current and planned coal-fired power plants in India," *Proceedings of the National Academy of Sciences*, 2021, *118* (5).

Currie, Janet and Matthew Neidell, "Air pollution and infant health: what can we learn from California's recent experience?," *The Quarterly Journal of Economics*, 2005, *120* (3), 1003–1030.

_ **and Reed Walker**, "Traffic congestion and infant health: Evidence from E-ZPass," *American Economic Journal: Applied Economics*, 2011, *3* (1), 65–90.

_ **and Tom Vogl**, "Early-Life Health and Adult Circumstance in Developing Countries," *Annual Review of Economics*, 2013, *5* (1), 1–36.

_ **, Lucas Davis, Michael Greenstone, and Reed Walker**, "Environmental Health Risks and Housing Values: Evidence from 1,600 Toxic Plant Openings and Closings," *American Economic Review*, February 2015, *105* (2), 678–709.

Dandona, Rakhi, G Anil Kumar, Nathaniel J Henry, Vasna Joshua, Siddarth Ramji, Subodh S Gupta, Deepti Agrawal, Rashmi Kumar, Rakesh Lodha, Matthews Mathai et al., "Subnational mapping of under-5 and neonatal mortality trends in India: the Global Burden of Disease Study 2000–17," *The Lancet*, 2020, *395* (10237), 1640–1658.

der Goltz, Jan Von and Prabhat Barnwal, "Mines: The local wealth and health effects of mineral mining in developing countries," *Journal of Development Economics*, 2019, *139*, 1–16.

Deryugina, Tatyana, Garth Heutel, Nolan H Miller, David Molitor, and Julian Reif, "The mortality and medical costs of air pollution: Evidence from changes in wind direction," *American Economic Review*, 2019, *109* (12), 4178–4219.

Deschênes, Olivier and Michael Greenstone, "The economic impacts of climate change: evidence from agricultural output and random fluctuations in weather," *American economic review*, 2007, *97* (1), 354–385.

Donkelaar, Aaron Van, Randall V Martin, Michael Brauer, N Christina Hsu, Ralph A Kahn, Robert C Levy, Alexei Lyapustin, Andrew M Sayer, and David M Winker, "Global estimates of fine particulate matter using a combined geophysical-statistical method with information from satellites, models, and monitors," *Environmental science & technology*, 2016, *50* (7), 3762–3772.

Draxler, Roland R and GD Hess, "An overview of the HYSPLIT_4 modelling system for trajectories," *Australian meteorological magazine*, 1998, *47* (4), 295–308.

_ **, Barbara Stunder, Glenn Rolph, Ariel Stein, and Albion Taylor**, "HYSPLIT4 users's guide," Technical Report 2020.

Druckenmiller, Hannah and Solomon Hsiang, "Accounting for unobservable heterogeneity in cross section using spatial first differences," Technical Report, National Bureau of Economic Research 2018.

Duflo, Esther and Rohini Pande, "Dams," *The Quarterly Journal of Economics*, 2007, *122* (2), 601–646.

Fowlie, Mededith, Ed Rubin, and Catherine Write, "Declining power-plant emissions, co-benefits, and regulatory rebound," Technical Report 2023.

Government of India, "India's Updated First Nationally Determined Contribution Under Paris Agreement," Technical Report 2022.

Gulati, Sumeet, Krithi K Karanth, Nguyet Anh Le, and Frederik Noack, "Human casualties are the dominant cost of human–wildlife conflict in India," *Proceedings of the National Academy of Sciences*, 2021, *118* (8).

Gupta, Aashish and Dean Spears, "Health externalities of India's expansion of coal plants: Evidence from a national panel of 40,000 households," *Journal of Environmental Economics and Management*, 2017, *86*, 262–276.

Guttikunda, Sarath K and Puja Jawahar, "Atmospheric emissions and pollution from the coal-fired thermal power plants in India," *Atmospheric Environment*, 2014, *92*, 449–460.

Heblich, Stephan, Alex Trew, and Yanos Zylberberg, "East Side Story: Historical Pollution and Persistent Neighborhood Sorting," Discussion Paper Series, School of Economics and Finance 201613, School of Economics and Finance, University of St Andrews November 2016.

Henderson, J Vernon, Adam Storeygard, and David N Weil, "Measuring economic growth from outer space," *American economic review*, 2012, *102* (2), 994–1028.

Henneman, Lucas R. F., Christine Choirat, Cesunica Ivey, Kevin Cummiskey, and Corwin M. Zigler, "Characterizing population exposure to coal emissions sources in the United States using the HyADS model," *Atmospheric Environment*, April 2019, *203*, 271–280.

_ , Irene C. Dedoussi, Joan A. Casey, Christine Choirat, Steven R. H. Barrett, and Corwin M. Zigler, "Comparisons of simple and complex methods for quantifying exposure to individual point source air pollution emissions," *Journal of Exposure Science & Environmental Epidemiology*, July 2021, *31* (4), 654–663. Bandiera_abtest: a Cg_type: Nature Research Journals Number: 4 Primary_atype: Research Publisher: Nature Publishing Group.

Heo, Seonmin Will, Koichiro Ito, and Rao Kotamarthi, "International Spillover Effects of Air Pollution: Evidence from Mortality and Health Data," Technical Report, National Bureau of Economic Research 2023.

Hernandez-Cortes, Danae and Kyle C Meng, "Do environmental markets cause environmental injustice? Evidence from California's carbon market," *Journal of Public Economics*, 2023, *217*, 104786.

Herrnstadt, Evan, Anthony Heyes, Erich Muehlegger, and Soodeh Saberian, "Air pollution and criminal activity: Microgeographic evidence from Chicago," *American Economic Journal: Applied Economics*, 2021, *13* (4), 70–100.

International Energy Agency, *India Energy Outlook 2021* 2021.

Jayachandran, Seema, "Air quality and early-life mortality evidence from Indonesia's wildfires," *Journal of Human resources*, 2009, *44* (4), 916–954.

Kleibergen, Frank and Richard Paap, "Generalized reduced rank tests using the singular value decomposition," *Journal of econometrics*, 2006, *133* (1), 97–126.

Knittel, Christopher R, Douglas L Miller, and Nicholas J Sanders, "Caution, drivers! Children present: Traffic, pollution, and infant health," *Review of Economics and Statistics*, 2016, *98* (2), 350–366.

Komisarow, Sarah and Emily L Pakhtigian, "Are power plant closures a breath of fresh air? Local air quality and school absences," *Journal of Environmental Economics and Management*, 2022, p. 102569.

Kuminoff, Nicolai V., V. Kerry Smith, and Christopher Timmins, "The New Economics of Equilibrium Sorting and Policy Evaluation Using Housing Markets," *Journal of Economic Literature*, December 2013, *51* (4), 1007–62.

Landrigan, Philip J, Richard Fuller, Nereus J R Acosta, Olusoji Adeyi, Robert Arnold, Niladri (Nil) Basu, Abdoulaye Bibi Baldé, Roberto Bertollini, Stephan Bose-O'Reilly, Jo Ivey Boufford, Patrick N Breysse, Thomas Chiles, Chulabhorn Mahidol, Awa M Coll-Seck, Maureen L Cropper, Julius Fobil, Valentin Fuster, Michael Greenstone, Andy Haines, David Hanrahan, David Hunter, Mukesh Khare, Alan Krupnick, Bruce Lanphear, Bindu Lohani, Keith Martin, Karen V Mathiasen, Maureen A McTeer, Christopher J L Murray, Johanita D Ndahimananjara, Frederica Perera, Janez Potočnik, Alexander S Preker, Jairam Ramesh, Johan Rockström, Carlos Salinas, Leona D Samson, Karti Sandilya, Peter D Sly, Kirk R Smith, Achim Steiner, Richard B Stewart, William A Suk, Onno C P van Schayck, Gautam N Yadama, Kandeh Yumkella, and Ma Zhong, "The Lancet Commission on Pollution and Health," *The Lancet*, February 2018, *391* (10119), 462–512.

Lipscomb, Molly, A Mushfiq Mobarak, and Tania Barham, "Development effects of electrification: Evidence from the topographic placement of hydropower plants in Brazil," *American Economic Journal: Applied Economics*, 2013, *5* (2), 200–231.

Lu, Zifeng and David G Streets, "Increase in NO x emissions from Indian thermal power plants during 1996–2010: unit-based inventories and multisatellite observations," *Environmental Science & Technology*, 2012, *46* (14), 7463–7470.

_ , _ , Benjamin de Foy, and Nickolay A Krotkov, "Ozone Monitoring Instrument observations of interannual increases in SO2 emissions from Indian coal-fired power plants during 2005–2012," *Environmental science & technology*, 2013, *47* (24), 13993–14000.

MacQueen, James et al., "Some methods for classification and analysis of multivariate observations," in "Proceedings of the fifth Berkeley symposium on mathematical statistics and probability," Vol. 1 Oakland, CA, USA 1967, pp. 281–297.

Mays, G. T., R. J. Belles, B. R. Blevins, S. W. Hadley, T. J. Harrison, W. C. Jochem, B. S. Neish, O. A. Omitaomu, and A. N. Rose, "Application of Spatial Data Modeling and Geographical Information Systems (GIS) for Identification of Potential Siting Options for Various Electrical Generation Sources," Technical Report, Oak Ridge National Laboratory December 2011.

Mendelsohn, Robert, William D Nordhaus, and Daigee Shaw, "The impact of global warming on agriculture: a Ricardian analysis," *The American economic review*, 1994, pp. 753–771.

Ministry of Power, "National Electricity Plan (Volume I)," Technical Report 2018.

Morehouse, John and Edward Rubin, "Downwind and Out: The Strategic Dispersion of Power Plants and Their Pollution," Technical Report 2021.

Munshi, Kaivan and Mark Rosenzweig, "Networks and misallocation: Insurance, migration, and the rural-urban wage gap," *American Economic Review*, 2016, *106* (1), 46–98.

Murray, Christopher J L, Aleksandr Y Aravkin, Peng Zheng, Cristiana Abbafati, Kaja M Abbas, Mohsen Abbasi-Kangevari, Foad Abd-Allah, Ahmed Abdelalim, Mohammad Abdollahi, Ibrahim Abdollahpour, Kedir Hussein Abegaz, Hassan Abolhassani, Victor Aboyans, Lucas Guimarães Abreu, Michael R M Abrigo, Ahmed Abualhasan, Laith Jamal Abu-Raddad, Abdelrahman I Abushouk, and Maryam Adabi, "Global burden of 87 risk factors in 204 countries and territories, 1990–2019: a systematic analysis for the Global Burden of Disease Study 2019," *The Lancet*, October 2020, *396* (10258), 1223–1249.

Olea, José Luis Montiel and Carolin Pflueger, "A robust test for weak instruments," *Journal of Business & Economic Statistics*, 2013, *31* (3), 358–369.

Perera, Frederica and Julie Herbstman, "Prenatal environmental exposures, epigenetics, and disease," *Reproductive toxicology*, 2011, *31* (3), 363–373.

Planning Commission, "Indian Five Year Plan, 1961-66," Policy Document, Planning Commission, Government of India 1961.

Pullabhotla, Hemant K and Mateus Souza, "Air pollution from agricultural fires increases hypertension risk," *Journal of Environmental Economics and Management*, 2022, *115*, 102723.

Rosales-Rueda, Maria and Margaret Triyana, "The persistent effects of early-life exposure to air pollution evidence from the indonesian forest fires," *Journal of Human Resources*, 2019, *54* (4), 1037–1080.

Shearer, Christine, Matthew-Shah Neha, Lauri Myllyvirta, Aiqun Yu, and Ted Nace, *Boom and bust 2019*, Sierra Club, 2019.

_ , **Robert Fofrich, and Steven J Davis**, "Future CO2 emissions and electricity generation from proposed coal-fired power plants in India," *Earth's Future*, 2017, *5* (4), 408–416.

Trippi, Michael H and Susan J Tewalt, "Geographic information system (GIS) representation of coal-bearing areas in India and Bangladesh," Technical Report 2011.

Varadhan, Sudharshan, "Reuters: India asks utilities to not retire coal-fired power plants till 2030," 2023. Accessed: June 8th 2023.

Venkataraman, Chandra, Michael Brauer, Kushal Tibrewal, Pankaj Sadavarte, Qiao Ma, Aaron Cohen, Sreelekha Chaliyakunnel, Joseph Frostad, Zbigniew Klimont, Randall V Martin et al., "Source influence on emission pathways and ambient PM 2.5 pollution over India (2015–2050)," *Atmospheric Chemistry and Physics*, 2018, *18* (11), 8017–8039.

Wen, Jeff, Patrick Baylis, Judson Boomhower, and Marshall Burke, "Quantifying fire-specific smoke severity," 2023.